The total creep of viscoelastic composites under hydrostatic or antiplane loading

V. Vinogradov *, G. W. Milton

Department of Mathematics, University of Utah, 155 S 1400 E, Salt Lake City, UT 84112, USA

Abstract

The problem of bounding the total creep (or total stress relaxation) of a composite made of two linear viscoelastic materials and subjected to a constant hydrostatic or antiplane loading is considered. It is done by coupling the immediate and the relaxed responses of the composite, which are pure elastic. The coupled bounds provide the possible range of the total deformation at infinite time as a function of the initial deformation of the composite. For antiplane shear existing bounds for coupled two dimensional conductivity yield the required coupled bounds, and these are attained by doubly coated cylinder assemblages. The translation method is used to couple the effective bulk moduli of a viscoelastic composite at zero and infinite time. A number of microgeometries are found to attain the bulk modulus bounds. It is shown that the Hashin's composite sphere assemblage does not necessarily correspond to the maximum or minimum overall creep, although it necessarily attains the bounds for effective bulk moduli. For instance, there are cases when the doubly coated sphere microstructure or some special polycrystal arrangements attain the bounds on the total creep.

Key words: Viscoelasticity, Creep, Composites, Coupled bounds, Translation method.

1 Introduction

Most materials exhibit some viscoelastic response: polymers, wood, glasses, bone tissue, metals at high temperature and many other substances have a delayed response

* Corresponding author.
Email addresses: vladim@math.utah.edu (V. Vinogradov), milton@math.utah.edu (G. W. Milton).

to applied loadings. Despite the prevalence of viscoelastic behavior comparatively little is known about the viscoelastic properties of composites, given the viscoelastic properties of the constituent phases. To make progress on this problem we will address the case of linear viscoelasticity where the loadings are small and the geometric deformation of the material under creep is also small.

If a linear viscoelastic homogeneous material is subjected to a cyclic loading with a certain frequency, one can use the correspondence principle (see Hashin, 1970a,b; Christensen, 1971) to obtain the response of the material, when complex moduli should be substituted into an elastic solution instead of real ones. In this case the complex moduli are functions of the frequency of the applied load. The response of a viscoelastic composite material to an oscillating load is described by effective complex moduli which are functions of the frequency as well. The correspondence principle implies that a formula for the effective moduli that is valid when the constituent moduli are real, will also be valid when the constituent moduli are complex. Its rigorous justification uses the fact [established by Bergman (1978a,b); Milton (1981a); Golden and Papanicolaou (1983) for antiplane elasticity and by Kantor and Bergman (1984) for elasticity] that the effective moduli are analytic functions of the constituent moduli, with these analytic functions having special properties. For example, the effective antiplane shear modulus of a columnar structure with a checkerboard microgeometry is $\sqrt{\mu_1\mu_2} = \mu_2\sqrt{\mu_1/\mu_2}$ where μ_1 and μ_2 are the shear moduli of the constituent phases occupying the black and white regions of the checkerboard. To use the correspondence principle one needs to know where to place the branch cut of the function. The known analytic properties of the effective antiplane shear modulus force one to place the branch cut where μ_1/μ_2 is real and negative.

The analytic properties led Milton (1981a,b) and Bergman (1982) in independent work to obtain bounds on the complex elastic moduli of a two-phase viscoelastic composite for antiplane elasticity (or more precisely for the mathematically equivalent complex conductivity problem). These bounds confined the effective antiplane shear modulus to lie in a lens-shaped region of the complex plane, with the size of the lens dependent on the extent of information available about the composite microgeometry. Sharp bounds were obtained by Milton (1981b) in the particular case of a transversely isotropic composite with prescribed volume fractions of the two components: in this case any point on the boundary of the lens is attained when the microgeometry consists of an appropriate doubly coated cylinder assemblage.

A different approach to obtaining bounds on complex moduli was initiated following the discovery by Cherkaev and Gibiansky (1994) of a variational principle for media with complex moduli. Based on this variational principle, bounds on the complex bulk and shear moduli of a viscoelastic composites were obtained in a series of papers by Gibiansky and Milton (1993); Milton and Berryman (1997) and Gibiansky, Milton, and Berryman (1999) using both Hashin–Shtrikman method and the translation method.

However, if an applied load is suddenly applied at some instant of time and then held constant, a homogeneous material will demonstrate some immediate elastic response and then continuous creep, asymptotically approaching the relaxed value of the response. A viscoelastic composite will demonstrate similar behavior, in which the creep depends on the phase viscoelastic properties and the composite structure. A random heterogeneous viscoelastic medium can exhibit a quite different response in time than its constituent phases. Even for the simple case where the composite material is subjected to a constant load instantly applied to the boundary, it is not clear what response one should expect from the composite after waiting a while. It is obvious that the initial response of the materials can be easily measured, but measurement of the relaxed moduli requires a long-term experiment. The question arises: Can one use this information about the initial response to predict the composite behavior after a long (infinite) period of time. One can also wonder about what is the minimum (or maximum) creep (or relaxation) that can be achieved from a mixture of two viscoelastic materials, and what are the microgeometries of the composite that have the minimum/maximum creep.

In the current paper an effort is made to answer these questions by bounding the effective bulk modulus of the composite at infinite time when the effective bulk modulus at time zero is known. Using the coupled bounds of Milton (1981b) for the two-dimensional conductivity problem, we will also obtain sharp bounds on the effective antiplane shear modulus of the composite at infinite time when the effective antiplane shear modulus at time zero is known. Coupled bounds correlating different properties of a composite material have been investigated in a number of papers. Indeed, knowledge of any effective property of a random heterogeneous media reflects some information on its microstructure. Thus one can use this information to estimate or to bound another effective property, which is more difficult to measure, and the bounds are expected to be much more tight than without this information. As examples of such bounds we mention works by Prager (1969); Bergman (1978b); Milton (1981a,b); Berryman and Milton (1988); Cherkaev and Gibiansky (1992, 1993); Clark and Milton (1995) and papers of Gibiansky and Torquato (1993, 1995, 1996a,b) where various cross-properties relations were obtained.

It is also known that a viscoelastic material which is not a liquid behaves as a pure elastic material at zero and infinite time (Hashin, 1983). Moreover, the moduli at zero time correspond to the complex moduli observed when an oscillating load with infinite frequency is applied to the material, while the relaxed moduli correspond to zero frequency or static load. The complex moduli become real at these limits. As an illustration of this correspondence one can consider a simple “dash-pot model” of an idealized linear viscoelastic solid, with a first spring in series with an composite element, comprised of a damping element in parallel with a second spring. If the frequency of oscillations is very high, which corresponds to a high deformation rate, the damping element becomes rigid and the elastic modulus is equal to the stiffness of the first spring. The damping element is rigid as well at the initial moment of the material deformation under a suddenly applied load, but its stiffness vanishes with time, which also occurs if a quasi-static load is applied. In this latter case the stiffness equals the stiffness of the two springs in series. Thus, the problem of correlating the immediate and relaxed elastic moduli of a composite is equivalent to coupling two pure elastic states that are characterized by changing the elastic moduli of the phases from the immediate to the relaxed ones. From this point of view, the paper by Gibiansky and Torquato (1996b) is most relevant to the present work. They obtained bounds coupling two special elastic problems, correlating the effective elastic moduli of an isotropic two-phase composite with the effective elastic moduli of a composite with the same microstructure, but with the phases interchanged. At the end of Section 4.1.2 we will see that their coupled bounds for the effective bulk modulus are a special case of our coupled bounds.

2 Summary of results

Our results are bounds correlating the effective bulk moduli κ_*^A and κ_*^B for two composites sharing the same microgeometry but having different elastic moduli of the two constituent phases, i.e. having bulk moduli κ_i^A, κ_i^B and shear moduli μ_i^A, μ_i^B in phase i, $i = 1, 2$. As applied to viscoelasticity, let us first consider two linear viscoelastic materials subjected to a constant hydrostatic stress. Let κ_i^A, μ_i^A represent the immediate elastic moduli of the materials $i = 1, 2$ at zero time (infinite frequency) and κ_i^B, μ_i^B represent the relaxed moduli of the phases at infinite time (zero frequency). Given the immediate effective bulk modulus κ_*^A of the mixture, the relaxed effective modulus κ_*^B can be bounded as follows.

The bounds are simply expressed in terms of a parameter y_κ which can be obtained from the effective bulk modulus κ_* via the Y-transform, which for the immediate and the relaxed moduli respectively is defined by

$$\begin{aligned} y_\kappa^A &= -f_2\kappa_1^A - f_1\kappa_2^A - \frac{f_1 f_2(\kappa_1^A - \kappa_2^A)^2}{\kappa_*^A - f_1\kappa_1^A - f_2\kappa_2^A}, \\ y_\kappa^B &= -f_2\kappa_1^B - f_1\kappa_2^B - \frac{f_1 f_2(\kappa_1^B - \kappa_2^B)^2}{\kappa_*^B - f_1\kappa_1^B - f_2\kappa_2^B}. \end{aligned} \tag{2.1}$$

Here f_1 and f_2 are the respective volume fractions of phases 1 and 2.

We distinguish the case when the material constants μ_1^A, μ_1^B and μ_2^A, μ_2^B satisfy the relation

$$(\mu_2^A - \mu_1^A)(\mu_2^B - \mu_1^B) \leq 0, \tag{2.2}$$

which we call the "*badly ordered case*" from the case when these constants satisfy the opposite relation

$$(\mu_2^A - \mu_1^A)(\mu_2^B - \mu_1^B) \geq 0, \tag{2.3}$$

which will be called the "*well ordered case*". Notice, that despite the fact that our aim is to obtain estimates for the effective bulk modulus, the ordering is defined by relations amongst the shear moduli.

In the badly ordered case the *upper bound* is given by a straight line joining the points $P_1 = \frac{4}{3}(\mu_1^A, \mu_1^B)$ and $P_2 = \frac{4}{3}(\mu_2^A, \mu_2^B)$ in the (y_κ^A, y_κ^B) plane:

$$\frac{y_\kappa^A}{c_1} + \frac{y_\kappa^B}{c_2} = 1, \tag{2.4}$$

where the coefficients c_1 and c_2 are defined by

$$c_1 = \frac{4}{3}\frac{\mu_1^A\mu_2^B - \mu_2^A\mu_1^B}{\mu_2^B - \mu_1^B}, \quad c_2 = -\frac{4}{3}\frac{\mu_1^A\mu_2^B - \mu_2^A\mu_1^B}{\mu_2^A - \mu_1^A}.$$

The *lower bound* is a hyperbola joining P_1 and P_2:

$$(\frac{y_\kappa^A}{d_1} - 1)(\frac{y_\kappa^B}{d_2} - 1) = 1, \tag{2.5}$$

where

$$d_1 = \frac{4}{3}\frac{\mu_1^A\mu_2^A(\mu_2^B - \mu_1^B)}{\mu_1^A\mu_2^B - \mu_2^A\mu_1^B}, \quad d_2 = -\frac{4}{3}\frac{\mu_1^B\mu_2^B(\mu_2^A - \mu_1^A)}{\mu_1^A\mu_2^B - \mu_2^A\mu_1^B}.$$

This hyperbola becomes a straight line when mapped to the $(1/y_\kappa^A, 1/y_\kappa^B)$ plane:

$$\frac{d_1}{y_\kappa^A} + \frac{d_2}{y_\kappa^B} = 1. \tag{2.6}$$

For the well-ordered case one should plot four curves joining P_1 and P_2: two of the curves are given by (2.5) and (2.4), while the remaining two curves are best represented in a parametric form. One curve has the parametric form:

$$\begin{aligned} y_\kappa^A(\xi) &= \frac{4}{3}\frac{f_2\mu_1^A\left(3\kappa_1^A + 4\mu_2^A\right)(1-\xi) + \left(3\kappa_1^A + 4\mu_1^A\right)\mu_2^A\xi}{f_2\left(3\kappa_1^A + 4\mu_2^A\right)(1-\xi) + \left(3\kappa_1^A + 4\mu_1^A\right)\xi}, \\ y_\kappa^B(\xi) &= \frac{4}{3}\frac{f_2\mu_1^B\left(3\kappa_1^B + 4\mu_2^B\right)(1-\xi) + \left(3\kappa_1^B + 4\mu_1^B\right)\mu_2^B\xi}{f_2\left(3\kappa_1^B + 4\mu_2^B\right)(1-\xi) + \left(3\kappa_1^B + 4\mu_1^B\right)\xi}, \end{aligned} \tag{2.7}$$

where $0 \le \xi \le 1$ parameterizes the curve. The other curve has a parametric form analogous to (2.7) but with the roles of the phases switched, i.e. with the indices 1 and 2 swapped. The bounds are given by the outermost pair of these four curves.

The points P_1 and P_2 that all the curves pass through correspond to the Hashin–Shtrikman bounds (Hashin and Shtrikman, 1963) attained by the well-known composite sphere assemblage of Hashin (1962). There are three additional points P_3,

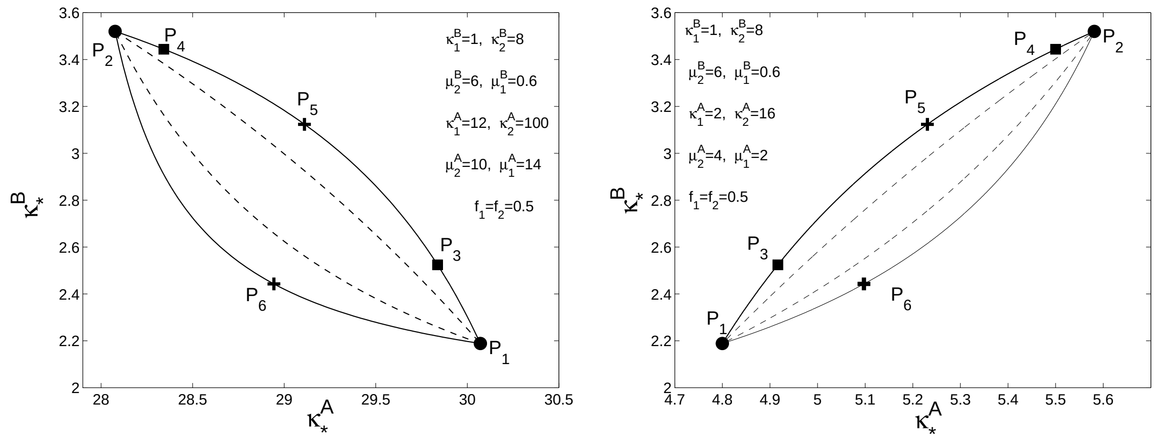

(a) (b)

Fig. 1. Examples of coupled bounds correlating the effective relaxed bulk modulus κ_*^B and the immediate bulk modulus κ_*^A for the badly-ordered case (a) and the well-ordered case (b). The dashed lines correspond to the doubly coated sphere assemblage. Points P_1 and P_2 correspond to the Hashin–Shtrikman bounds. Points $P_3 - P_6$ on the bounding curves correspond to special polycrystal assemblages described in Section 5.

P_4 and P_5 on the bound defined by (2.4) and one point P_6 on (2.6) that are attained by known microgeometries of some special polycrystal assemblages described in Section 5. The bounds given by (2.7) correspond to assemblages of doubly coated spheres and ξ corresponds to the proportion of phase 1 in the core of each doubly coated sphere. Examples of the coupled bounds for the different ordered composite materials are shown in Figures 1 and 2.

Since the total stress relaxation of the composite subjected to a hydrostatic deformation is proportional to the change in the effective bulk modulus from zero time to infinity $(\kappa_*^B - \kappa_*^A)$, one needs to find bounds on $\max\{\kappa_*^B - \kappa_*^A\}$ and $\min\{\kappa_*^B - \kappa_*^A\}$ from the coupled bounds. Graphically, these bounds are obtained by plotting two straight lines of unit slope tangent to the lens-shaped region enclosed by the coupled bounds and measuring the distance from the points of their intersection with the κ_*^B axis to the origin of the coordinate system (see Figure 3). Similarly, the total creep (dilatation) of the composite due to a hydrostatic loading is defined by the change in the effective compliance from zero time to infinity $(1/\kappa_*^B - 1/\kappa_*^A)$. Thus, the bounds on $\max\{1/\kappa_*^B - 1/\kappa_*^A\}$ and $\min\{1/\kappa_*^B - 1/\kappa_*^A\}$ correspond to points on the coupled bounds plotted in the $(1/\kappa_*^A, 1/\kappa_*^B)$ plane, see Figure 3.

The points on the coupled bounds that correspond to the maximum or minimum creep or stress relaxation (when realizable) define the microgeometries that attain the extreme values of the these functions. An example of the maximum and minimum total creep as a function of phase volume fractions and corresponding microgeometries are shown in Figure 4. In the badly ordered case the bounds on the total creep or total relaxation necessarily correspond to the Hashin–Shtrikman points P_1 and P_2 and thus are attained by assemblages of singly coated spheres. However the coupled

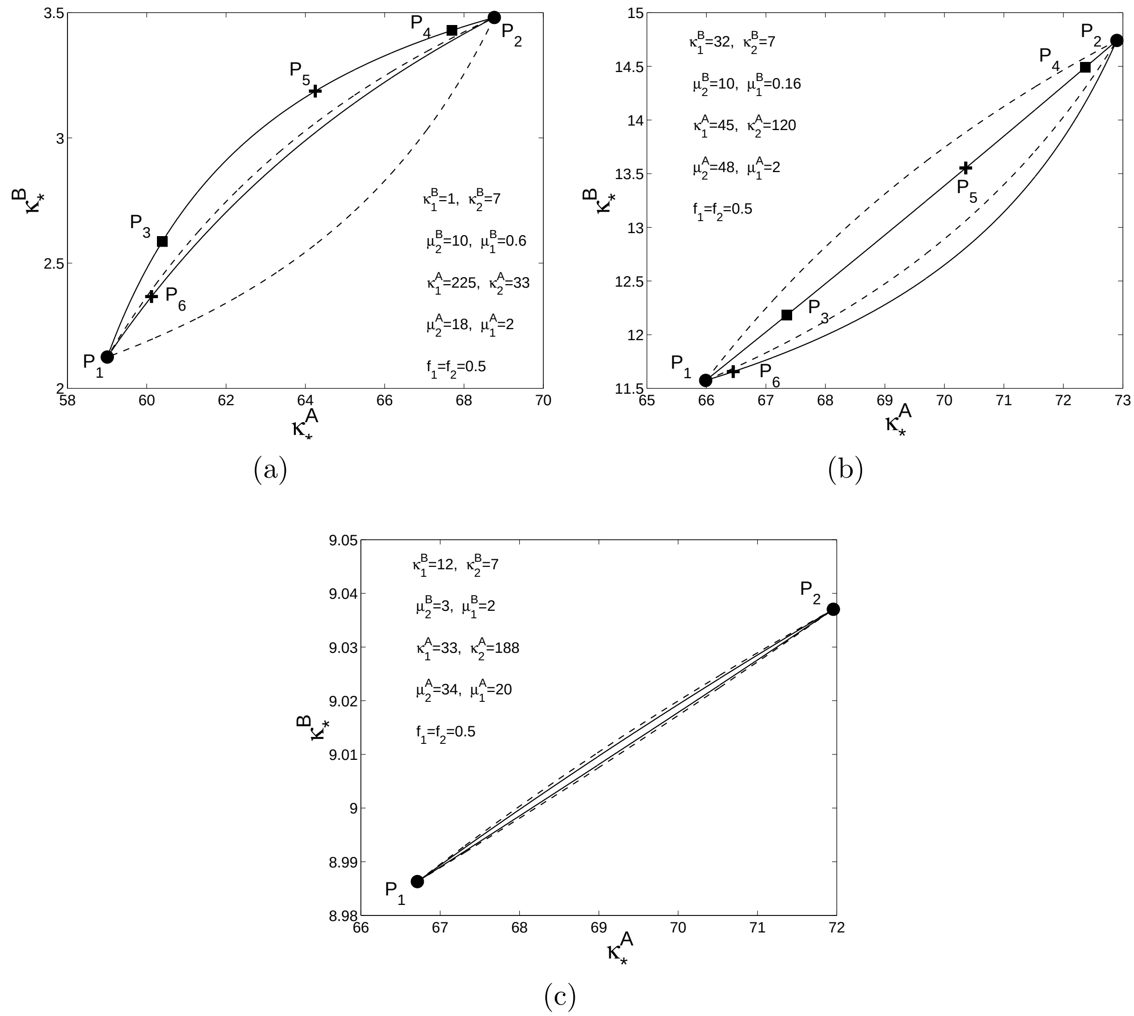

Fig. 2. Additional examples of coupled bounds correlating the effective relaxed bulk modulus κ_*^B and the immediate bulk modulus κ_*^A for the well-ordered case. The dashed lines correspond to the doubly coated sphere assemblage. It can be seen that the doubly coated assemblage can attain one of the bounds – the lower bound in (a) and the upper bound in (b) or both bounds simultaneously (c).

bounds are still useful in this case as they provide correlations between the total creep or total relaxation and the effective bulk modulus at zero time.

Using the mathematical equivalency of the antiplane elastic problem and two-dimensional conductivity problem one can adapt the known coupled bounds correlating the effective conductivities derived by Milton (1981b) to the antiplane elastic problem. Then the effective shear modulus at infinite time μ_*^B is bounded by the following values denoted as μ_{1*}^B and μ_{2*}^B, given the effective antiplane shear modulus at zero time μ_*^A:

$$\begin{aligned}
\mu_{1*}^B = &\ \ \mu_2^B \frac{(f_1\mu_1^B + f_2\mu_2^B + \mu_1^B)(\mu_1^B + \mu_2^B) - \beta_2(\mu_1^B - \mu_2^B)^2}{(f_2\mu_1^B + f_1\mu_2^B + \mu_2^B)(\mu_1^B + \mu_2^B) - \beta_2(\mu_1^B - \mu_2^B)^2},\\
\mu_{2*}^B = &\ \ \mu_1^B \frac{(f_1\mu_1^B + f_2\mu_2^B + \mu_2^B)(\mu_1^B + \mu_2^B) - \beta_1(\mu_1^B - \mu_2^B)^2}{(f_2\mu_1^B + f_1\mu_2^B + \mu_1^B)(\mu_1^B + \mu_2^B) - \beta_1(\mu_1^B - \mu_2^B)^2},
\end{aligned} \tag{2.8}$$

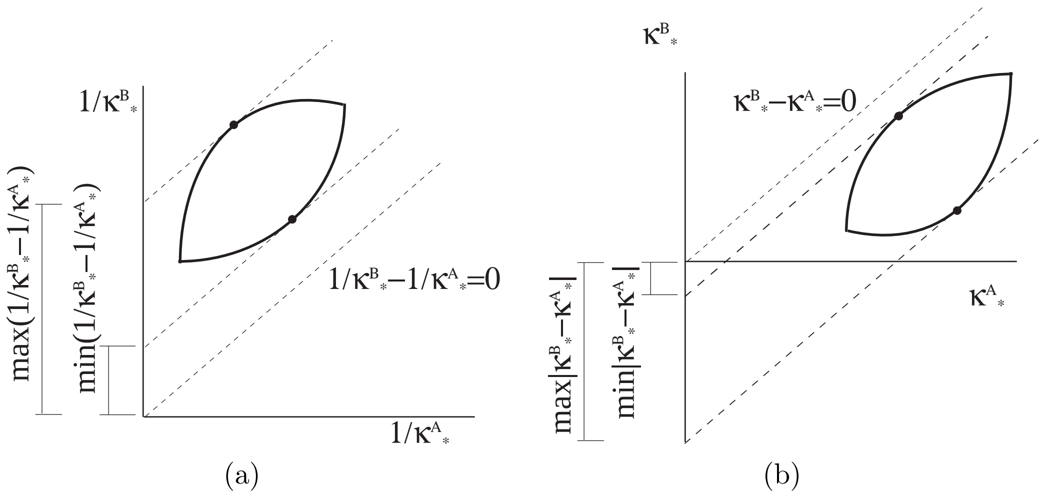

Fig. 3. Schematic illustration of the procedure for obtaining bounds on the total creep (a) and the total stress relaxation (b).

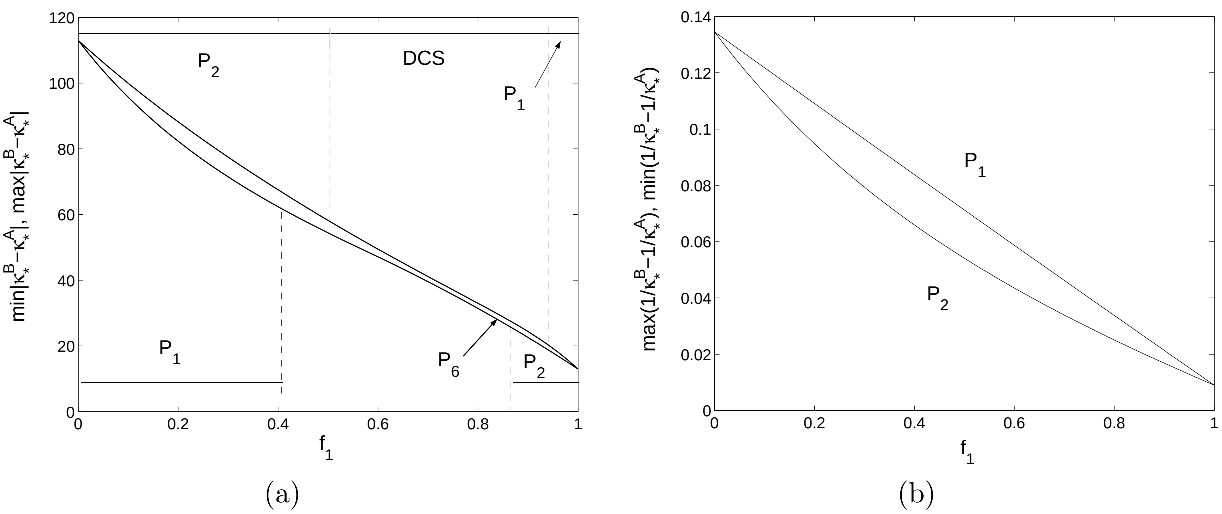

Fig. 4. Examples of the bounds on the total stress relaxation (a) and the total creep (b) as functions of the phase volume fraction in the well ordered case shown in Figure 2(b). The ranges of the volume fraction f_1 for which the corresponding microgeometry is known are indicated in the upper and lower part of the graph for the upper and lower bound, respectively: P_1, P_2 and P_3 correspond to the points in Figure 2(b) and DCS denotes the doubly coated sphere assemblage.

where the parameters β_1 and β_2 are defined as

$$\begin{aligned}\beta_1 = &\quad \frac{(\mu_1^A+\mu_2^A)[(f_2\mu_1^A+f_1\mu_2^A+\mu_1^A)+2f_2\mu_1(\mu_1^A-\mu_2^A)/(\mu_*^A-\mu_1^A)]}{(\mu_1^A-\mu_2^A)^2},\\ \beta_2 = &\quad \frac{(\mu_1^A+\mu_2^A)[(f_2\mu_1^A+f_1\mu_2^A+\mu_1^A)-2f_1\mu_2(\mu_1^A-\mu_2^A)/(\mu_*^A-\mu_2^A)]}{(\mu_1^A-\mu_2^A)^2}.\end{aligned} \tag{2.9}$$

The bounds correspond to doubly coated cylinder assemblages. The bounds on the total creep and the total stress relaxation of the composite material are defined in a

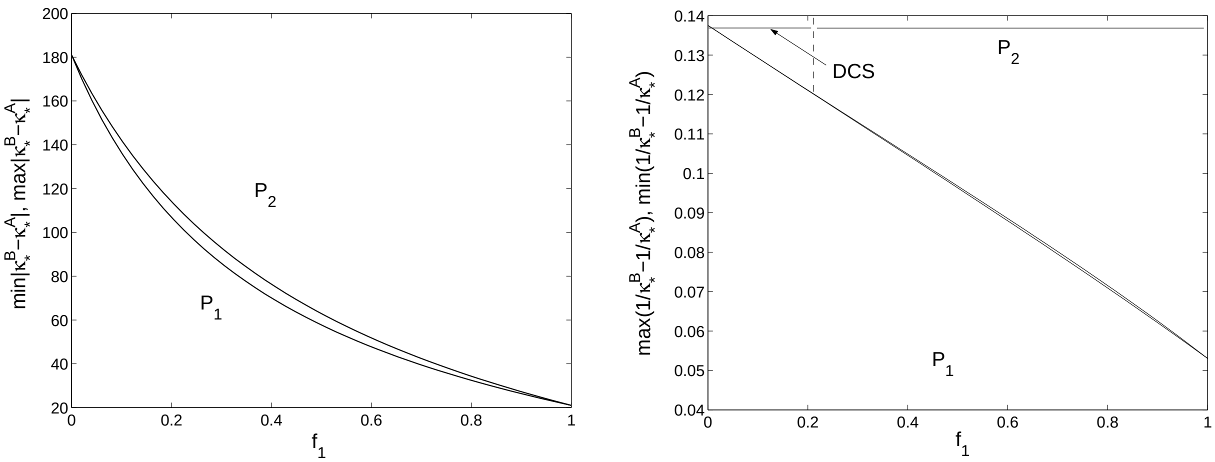

(a) (b)

Fig. 5. Examples of the bounds on the total stress relaxation (a) and the total creep (b) as functions of the phase volume fraction in the well ordered case shown in Figure 2(c). The ranges of the volume fraction f_1 for which the corresponding microgeometry is known are indicated in the upper and lower part of the graph for the upper and lower bound, respectively: P_1, P_2 correspond to the points in Figure 2(c) and DCS denotes the doubly coated sphere assemblage.

manner similar to the previous case of hydrostatic loading and therefore the transversely isotropic composites exhibiting the maximum or minimum total creep (or total stress relaxation) under antiplane loading are coated cylinder assemblages with either one or two coatings. Using the bounds of Cherkaev and Gibiansky (1992) one can extend these results to the antiplane viscoelastic response of anisotropic composites of two isotropic phases.

3 General formulation

Let us consider a statistically homogeneous or periodic composite material with a length scale of inhomogeneities much smaller than the length scale of the body. The composite is subjected to a homogeneous condition on the boundary S described by position vector $\boldsymbol{x}$ and unit normal $\boldsymbol{n}$ such that either a homogeneous displacement

$$\boldsymbol{u}(S) = \boldsymbol{\varepsilon}^0 \cdot \boldsymbol{x}\, H(t), \tag{3.1}$$

or a homogeneous traction

$$\mathbf{T}(S) = \boldsymbol{\tau}^0 \cdot \boldsymbol{n}\, H(t), \tag{3.2}$$

are applied. Here $\boldsymbol{\varepsilon}^0$ and $\boldsymbol{\tau}^0$ are constant strain and stress tensors and $H(t)$ is the Heaviside step function of time. Then it is obvious that the volume average strains are $\boldsymbol{\varepsilon}^0 H(t)$ in the former case and the average stresses are $\boldsymbol{\tau}^0 H(t)$ in the latter case and they remain constant for any time from zero to infinity.

As we described above, the two limiting states of zero and infinite time (cases A and B) are pure elastic. The state of any linear elastic body is described by the following local relations:

$$\boldsymbol{\varepsilon} = \frac{1}{2}\left(\nabla \boldsymbol{u} + (\nabla \boldsymbol{u})^T\right), \quad \boldsymbol{\tau} = \boldsymbol{\mathcal{C}}\,\boldsymbol{\varepsilon}, \quad \boldsymbol{\tau} = \boldsymbol{\tau}^T, \quad \nabla \cdot \boldsymbol{\tau} = 0, \tag{3.3}$$

where $\boldsymbol{\varepsilon}$ and $\boldsymbol{\tau}$ are the strain and stress tensors, $\boldsymbol{u}$ is the displacement vector and $\boldsymbol{\mathcal{C}}$ is the stiffness tensor. Here a superscript A or B indicates that the phases are considered at zero or infinite time, respectively. Similarly, the average fields in a composite material satisfy the relations:

$$\langle\boldsymbol{\varepsilon}\rangle = \frac{1}{2}\left(\langle\nabla \boldsymbol{u}\rangle + \langle\nabla \boldsymbol{u}\rangle^T\right), \quad \langle\boldsymbol{\tau}\rangle = \boldsymbol{\mathcal{C}}_*\,\langle\boldsymbol{\varepsilon}\rangle, \quad \langle\boldsymbol{\tau}\rangle = \langle\boldsymbol{\tau}\rangle^T, \quad \nabla \cdot \langle\boldsymbol{\tau}\rangle = 0, \tag{3.4}$$

where $\langle\cdot\rangle$ denotes volume averaging and $\boldsymbol{\mathcal{C}}_*$ is the effective stiffness tensor. If the boundary conditions (3.1) are prescribed, then the average strains are known in both cases $\langle\boldsymbol{\varepsilon}^A\rangle = \boldsymbol{\varepsilon}_0$ and $\langle\boldsymbol{\varepsilon}^B\rangle = \boldsymbol{\varepsilon}_0$. Alternatively, if the boundary conditions are given by (3.2), the average stresses are prescribed for the states A and B: $\langle\boldsymbol{\tau}^A\rangle = \boldsymbol{\tau}_0$ and $\langle\boldsymbol{\tau}^B\rangle = \boldsymbol{\tau}_0$.

The elastic strain energy density in a composite subjected to a uniform external displacement (3.1) is given by the quadratic form

$$W_\varepsilon = \frac{1}{2}\boldsymbol{\varepsilon}_0 \cdot \boldsymbol{\mathcal{C}}_*\,\boldsymbol{\varepsilon}_0 = \frac{1}{2}\langle\boldsymbol{\varepsilon}\rangle \cdot \boldsymbol{\mathcal{C}}_*\,\langle\boldsymbol{\varepsilon}\rangle = \inf_{\substack{\langle\boldsymbol{\varepsilon}\rangle = \boldsymbol{\varepsilon}_0; \\ \boldsymbol{\varepsilon} = \frac{1}{2}(\nabla\boldsymbol{u} + (\nabla\boldsymbol{u})^T)}} \frac{1}{2}\langle\boldsymbol{\varepsilon} \cdot \boldsymbol{\mathcal{C}}\,\boldsymbol{\varepsilon}\rangle, \tag{3.5}$$

where the minimization is over all fields $\boldsymbol{\varepsilon}$ satisfying the constraints and the dot denotes the appropriate inner product, in this case, for any two possibly complex matrices $\mathcal{A}$ and $\mathcal{B}$, $\mathcal{A} \cdot \mathcal{B} = \mathrm{Tr}(\mathcal{A}^H\mathcal{B})$ where $\mathcal{A}^H$ is the Hermitian conjugate of $\mathcal{A}$. It is convenient to work directly with the displacement gradient $\boldsymbol{\zeta}(\boldsymbol{x}) = \nabla\boldsymbol{u}(\boldsymbol{x})$ rather than with the strain, because as recognized by Cherkaev and Gibiansky (1993) one can then use a wider class of quasiconvex functions (that include Null-Lagrangians) to obtain bounds using the translation method. Accordingly, the energy (3.5) can now be rewritten in terms of $\boldsymbol{\zeta}$

$$W_\zeta = \frac{1}{2}\boldsymbol{\zeta}_0 \cdot \boldsymbol{\mathcal{C}}_*\,\boldsymbol{\zeta}_0 = \frac{1}{2}\langle\boldsymbol{\zeta}\rangle \cdot \boldsymbol{\mathcal{C}}_*\langle\boldsymbol{\zeta}\rangle = \inf_{\boldsymbol{\zeta} = \nabla\boldsymbol{u}} \frac{1}{2}\langle\boldsymbol{\zeta} \cdot \boldsymbol{\mathcal{C}}\,\boldsymbol{\zeta}\rangle. \tag{3.6}$$

Notice that the antisymmetric part of matrix $\boldsymbol{\zeta}(\boldsymbol{x})$ has no influence on the quadratic form (3.5), because it vanishes when multiplied by the symmetric stiffness tensor.

The complementary energy of a composite subjected to a uniform traction on the boundary (3.2), is given by the quadratic form

$$W_\tau = \frac{1}{2}\boldsymbol{\tau}_0 \cdot \boldsymbol{\mathcal{S}}_*\,\boldsymbol{\tau}_0 = \frac{1}{2}\langle\boldsymbol{\tau}\rangle \cdot \boldsymbol{\mathcal{S}}_*\,\langle\boldsymbol{\tau}\rangle = \inf_{\substack{\langle\boldsymbol{\tau}\rangle = \boldsymbol{\tau}_0; \\ \boldsymbol{\tau} = \boldsymbol{\tau}^T,\ \nabla\cdot\boldsymbol{\tau} = 0}} \frac{1}{2}\langle\boldsymbol{\tau} \cdot \boldsymbol{\mathcal{S}}\,\boldsymbol{\tau}\rangle. \tag{3.7}$$

In order to obtain the best possible lower bound on the effective bulk stiffness one should minimize the complementary energy by varying the microgeometry of the composite. In this case the functional to be minimized is

$$I_\tau \equiv W_\tau. \tag{3.8}$$

Conversely, minimization of the functional

$$I_\zeta \equiv W_\zeta, \tag{3.9}$$

leads to the best possible upper bound on the effective bulk stiffness of the composite.

3.1 Translation bounds and the Y-tensor

In our analysis we will use the translation method, or equivalently the method of compensated compactness, to find bounds associated with minimizing appropriate functionals. The method of compensated compactness was first introduced by Tartar and Murat (Tartar, 1979a,b; Murat and Tartar, 1985), as a means for bounding the weak limit of a field constrained to take values in a certain set and satisfying some linear homogeneous differential constraints. A related energy based variational method, now called the translation method, was independently developed by Lurie and Cherkaev (1984, 1986). In the 1908's both groups used their newly developed methods to obtain sharp bounds on the effective conductivity tensor of a composite of two isotropic phases, generalizing the well-known Hashin–Shtrikman bounds (Hashin and Shtrikman, 1962) to anisotropic composites. Later the methods were developed to treat various effective properties. A detailed description of the methods and additional references can be found in the books of Cherkaev (2000) and Milton (2002): see in particular Section 25.1 of the latter book. Since for linear composites both methods are basically similar, we will focus on describing the translation method.

Briefly speaking, the translation method as applied to minimization of the functional (3.6) replaces the differential constraints on the fields by their integral corollaries in the form

$$\langle \boldsymbol{\zeta} \cdot \boldsymbol{\mathcal{T}}\, \boldsymbol{\zeta} \rangle \geq \langle \boldsymbol{\zeta} \rangle \cdot \boldsymbol{\mathcal{T}} \langle \boldsymbol{\zeta} \rangle, \tag{3.10}$$

which hold for every periodic field $\boldsymbol{\zeta} = \nabla \boldsymbol{u}$ for some self-adjoint matrices $\boldsymbol{\mathcal{T}}$ called "translation matrices". Functions that possess this property are usually called quadratic quasiconvex functions. In our analysis we will use the quasiconvexity test of Tartar (1979a) and Murat and Tartar (1985) who found that $\boldsymbol{\mathcal{T}}$ is quasiconvex, if any only if it satisfies the inequality

$$\hat{\boldsymbol{\zeta}}(\boldsymbol{k}) \cdot \boldsymbol{\mathcal{T}} \hat{\boldsymbol{\zeta}}(\boldsymbol{k}) \geq 0, \qquad \text{for} \quad \boldsymbol{k} \neq 0, \tag{3.11}$$

for all matrices $\hat{\boldsymbol{\zeta}}(\boldsymbol{k})$ that correspond to the Fourier-components of the gradient of some displacement vector field, in which $\boldsymbol{k}$ is the wavevector, i.e. for all rank 1 matrices

$\hat{\boldsymbol{\zeta}}(\boldsymbol{k})$. As Murat and Tartar observed, this quasiconvexity test easily generalizes to fields satisfying other linear differential constraints.

Replacing in (3.6) the differential constraints with the integral constraints leads to the inequality,

$$W_\zeta = \frac{1}{2}\boldsymbol{\zeta}_0 \cdot \boldsymbol{\mathcal{C}}_* \,\boldsymbol{\zeta}_0 \geq \inf_{\substack{\langle\boldsymbol{\zeta}\rangle=\boldsymbol{\zeta}_0;\\ \langle\boldsymbol{\zeta}\boldsymbol{\mathcal{T}}\boldsymbol{\zeta}\rangle\geq\boldsymbol{\zeta}_0\boldsymbol{\mathcal{T}}\boldsymbol{\zeta}_0}} \frac{1}{2}\langle\boldsymbol{\zeta}\cdot\boldsymbol{\mathcal{C}}\,\boldsymbol{\zeta}\rangle. \tag{3.12}$$

By introducing a non-negative Lagrange multiplier $c \geq 0$ to evaluate the above constrained infimum, standard analysis shows that (3.12) reduces to the following lower bound on the minimum value of the functional $I_\zeta = W_\zeta$:

$$W_\zeta = \frac{1}{2}\boldsymbol{\zeta}_0 \cdot \boldsymbol{\mathcal{C}}_* \,\boldsymbol{\zeta}_0 \geq \frac{1}{2}\boldsymbol{\zeta}_0 \cdot [c\boldsymbol{\mathcal{T}} + \langle(\boldsymbol{\mathcal{C}}(\boldsymbol{x}) - c\boldsymbol{\mathcal{T}})^{-1}\rangle^{-1}]\,\boldsymbol{\zeta}_0, \tag{3.13}$$

where we have assumed that c is chosen so that

$$\boldsymbol{\mathcal{C}}(\boldsymbol{x}) - c\boldsymbol{\mathcal{T}} \geq 0, \tag{3.14}$$

at any location $\boldsymbol{x}$. By redefining $\boldsymbol{\mathcal{T}}$ if necessary we can assume without loss of generality that $c = 1$ in which case the above constraint becomes one on $\boldsymbol{\mathcal{T}}$ directly:

$$\boldsymbol{\mathcal{C}}(\boldsymbol{x}) - \boldsymbol{\mathcal{T}} \geq 0. \tag{3.15}$$

Since the inequality (3.13) holds for all applied fields $\boldsymbol{\zeta}_0$ we deduce that the effective stiffness tensor must satisfy the associated bound

$$(\boldsymbol{\mathcal{C}}_* - \boldsymbol{\mathcal{T}})^{-1} \leq \langle(\boldsymbol{\mathcal{C}}(\boldsymbol{x}) - \boldsymbol{\mathcal{T}})^{-1}\rangle, \tag{3.16}$$

which defines a lower bound on $\boldsymbol{\mathcal{C}}_*$. Thus, the problem transforms to identifying the translations that possess the properties (3.10) and (3.15), and selecting those that produce the tightest bounds. Notice that the bound (3.16) is simply the harmonic mean bound applied to the translated tensors: hence the origin of the name translation method (Milton, 1990b).

For a two-phase composite the local stiffness tensor can be written in the form

$$\boldsymbol{\mathcal{C}}(\boldsymbol{x}) = \chi_1(\boldsymbol{x})\boldsymbol{\mathcal{C}}_1 + (1 - \chi_1(\boldsymbol{x}))\boldsymbol{\mathcal{C}}_2, \tag{3.17}$$

where the function $\chi_1(\boldsymbol{x})$ indicates whether the point $\boldsymbol{x}$ lies in the domain occupied by phase 1:

$$\chi_1(\boldsymbol{x}) = \begin{cases} 1, & \text{if } \boldsymbol{x} \in \Omega_1 \\ 0, & \text{otherwise.} \end{cases} \tag{3.18}$$

In this case the inequalities (3.15) are simply decomposed into

$$\boldsymbol{\mathcal{C}}_1 - \boldsymbol{\mathcal{T}} \geq 0, \quad \text{and} \quad \boldsymbol{\mathcal{C}}_2 - \boldsymbol{\mathcal{T}} \geq 0. \tag{3.19}$$

To simplify the analysis, it is convenient to introduce the Y-tensor $\boldsymbol{\mathcal{Y}}_*$ [see Milton (2002) for references] which is most simply defined by the linear relation between the volume averages of the fluctuation parts of the stress and strain fields in phase 1:

$$\Big\langle \chi_1(\boldsymbol{x})(\boldsymbol{\tau}(\boldsymbol{x}) - \langle \boldsymbol{\tau} \rangle) \Big\rangle = -\boldsymbol{\mathcal{Y}}_* \Big\langle \chi_1(\boldsymbol{x})(\boldsymbol{\varepsilon}(\boldsymbol{x}) - \langle \boldsymbol{\varepsilon} \rangle) \Big\rangle, \tag{3.20}$$

where $\boldsymbol{\tau}(\boldsymbol{x}) - \langle \boldsymbol{\tau} \rangle$ and $\boldsymbol{\varepsilon}(\boldsymbol{x}) - \langle \boldsymbol{\varepsilon} \rangle$ are fluctuation stress and strain fields, respectively. By substituting $\chi_1(\boldsymbol{x}) = 1 - \chi_2(\boldsymbol{x})$ one can see that the same relation holds in phase 2:

$$\Big\langle \chi_2(\boldsymbol{x})(\boldsymbol{\tau}(\boldsymbol{x}) - \langle \boldsymbol{\tau} \rangle) \Big\rangle = -\boldsymbol{\mathcal{Y}}_* \Big\langle \chi_2(\boldsymbol{x})(\boldsymbol{\varepsilon}(\boldsymbol{x}) - \langle \boldsymbol{\varepsilon} \rangle) \Big\rangle. \tag{3.21}$$

From this definition follows the explicit relation between the Y-tensor and the effective stiffness tensor of the composite:

$$\boldsymbol{\mathcal{Y}}_* = -f_1 \boldsymbol{\mathcal{C}}_1 - f_2 \boldsymbol{\mathcal{C}}_2 + f_1 f_2 (\boldsymbol{\mathcal{C}}_1 - \boldsymbol{\mathcal{C}}_2)[f_2 \boldsymbol{\mathcal{C}}_1 + f_1 \boldsymbol{\mathcal{C}}_2 - \boldsymbol{\mathcal{C}}_*]^{-1} (\boldsymbol{\mathcal{C}}_1 - \boldsymbol{\mathcal{C}}_2), \tag{3.22}$$

while its inverse provides the expression of the effective stiffness in terms of the Y tensor:

$$\boldsymbol{\mathcal{C}}_* = f_1 \boldsymbol{\mathcal{C}}_1 + f_2 \boldsymbol{\mathcal{C}}_2 - f_1 f_2 (\boldsymbol{\mathcal{C}}_1 - \boldsymbol{\mathcal{C}}_2)[f_2 \boldsymbol{\mathcal{C}}_1 + f_1 \boldsymbol{\mathcal{C}}_2 - \boldsymbol{\mathcal{Y}}_*]^{-1} (\boldsymbol{\mathcal{C}}_1 - \boldsymbol{\mathcal{C}}_2). \tag{3.23}$$

If two isotropic materials are mixed together to form an isotropic composite material, then the elastic stiffness tensor can be decomposed into its bulk and shear parts in the form

$$\boldsymbol{\mathcal{C}}_i = 3\kappa_i \boldsymbol{\Lambda}_h + 2\mu_i \boldsymbol{\Lambda}_s, \quad i = 1, 2, *, \tag{3.24}$$

where the isotropic fourth order tensors $\boldsymbol{\Lambda}_h$ and $\boldsymbol{\Lambda}_s$ are projection tensors onto the orthogonal subspaces of second-order tensors, comprised of tensors proportional to the identity tensor and trace-free tensors, respectively. The elements of these projection tensors are given by the relations

$$\{\boldsymbol{\Lambda}_h\}_{ijkl} = \frac{1}{3}\delta_{ij}\delta_{kl}, \qquad \{\boldsymbol{\Lambda}_s\}_{ijkl} = \frac{1}{2}\left(\delta_{ik}\delta_{jl} + \delta_{il}\delta_{jk}\right) - \frac{1}{3}\delta_{ij}\delta_{kl}, \tag{3.25}$$

where δ_{ij} is the Kronecker delta. Similarly the tensor $\boldsymbol{\mathcal{Y}}_*$ can be decomposed into

$$\boldsymbol{\mathcal{Y}}_* = 3y_\kappa \boldsymbol{\Lambda}_h + 2y_\mu \boldsymbol{\Lambda}_s, \tag{3.26}$$

where the bulk and shear y-parameters are given by the expressions

$$\begin{aligned} y_\kappa &= -f_2\kappa_1 - f_1\kappa_2 - \frac{f_1 f_2 (\kappa_1 - \kappa_2)^2}{\kappa_* - f_1\kappa_1 - f_2\kappa_2}, \\ y_\mu &= -f_2\mu_1 - f_1\mu_2 - \frac{f_1 f_2 (\mu_1 - \mu_2)^2}{\mu_* - f_1\mu_1 - f_2\mu_2}. \end{aligned} \tag{3.27}$$

To obtain the bounds on the Y-tensor one can start with the variational principle (3.6) and represent the displacement gradient $\boldsymbol{\zeta}(\boldsymbol{x})$ as a sum of three orthogonal fields

$$\boldsymbol{\zeta}(\boldsymbol{x}) = \boldsymbol{\zeta}_0 + \boldsymbol{\zeta}_1(\boldsymbol{x}) + \boldsymbol{\zeta}_2(\boldsymbol{x}), \tag{3.28}$$

where $\boldsymbol{\zeta}_1(\boldsymbol{x})$ is a field that is constant in each phase with zero volume average $\langle \boldsymbol{\zeta}_1(\boldsymbol{x}) \rangle = 0$, the field $\boldsymbol{\zeta}_2(\boldsymbol{x})$ has zero average in each phase $\langle \chi_i \boldsymbol{\zeta}_2(\boldsymbol{x}) \rangle = 0$ and the field sum $\boldsymbol{\zeta}_1(\boldsymbol{x}) + \boldsymbol{\zeta}_2(\boldsymbol{x})$ satisfies the same differential constraints as the field $\boldsymbol{\zeta}(\boldsymbol{x})$, i.e. is the gradient of some function. Then it can be shown that the variational principle (3.6) in terms of the Y-tensor assumes the form

$$\langle \boldsymbol{\zeta}_1(\boldsymbol{x}) \cdot \boldsymbol{\mathcal{Y}}_* \boldsymbol{\zeta}_1(\boldsymbol{x}) \rangle = \inf_{\boldsymbol{\zeta}_2} \langle \boldsymbol{\zeta}_2(\boldsymbol{x}) \cdot \boldsymbol{\mathcal{C}}(\boldsymbol{x}) \boldsymbol{\zeta}_2(\boldsymbol{x}) \rangle, \tag{3.29}$$

where the infimum is over all fields $\boldsymbol{\zeta}_2(\boldsymbol{x})$ such that $\boldsymbol{\zeta}_1(\boldsymbol{x}) + \boldsymbol{\zeta}_2(\boldsymbol{x})$ is a gradient and $\langle \chi_i \boldsymbol{\zeta}_2(\boldsymbol{x}) \rangle = 0, i = 1, 2$. The quasiconvexity of the translation tensor implies

$$0 \leq \left\langle \Big(\boldsymbol{\zeta}_1(\boldsymbol{x}) + \boldsymbol{\zeta}_2(\boldsymbol{x}) \Big) \cdot \boldsymbol{\mathcal{T}} \Big(\boldsymbol{\zeta}_1(\boldsymbol{x}) + \boldsymbol{\zeta}_2(\boldsymbol{x}) \Big) \right\rangle = \langle \boldsymbol{\zeta}_1(\boldsymbol{x}) \cdot \boldsymbol{\mathcal{T}} \boldsymbol{\zeta}_1(\boldsymbol{x}) \rangle + \langle \boldsymbol{\zeta}_2(\boldsymbol{x}) \cdot \boldsymbol{\mathcal{T}} \boldsymbol{\zeta}_2(\boldsymbol{x}) \rangle. \tag{3.30}$$

This inequality in conjunction with (3.15) and the variational principle (3.29) yields the following simple inequality that defines the bounds on the Y-tensor

$$\boldsymbol{\mathcal{Y}}_* + \boldsymbol{\mathcal{T}} \geq 0. \tag{3.31}$$

This bound is algebraically equivalent to the expression for the bound on the effective stiffness (3.16) given by the translation method, but is simpler to work with. We will call (3.31) the bound on the Y-tensor associated with minimization of the functional W_ζ.

Let us illustrate the method by obtaining the Hashin–Shtrikman lower bound on the effective bulk modulus of a two-phase linear elastic composite. [Francfort and Murat (1986) first discovered that the Hashin–Shtrikman bulk modulus bounds could be derived using the translation method, and subsequently the Hashin–Shtrikman shear modulus bounds were derived using the method by Milton (1990b,a)]. The moduli are decomposed according to (3.24). Let us take a rotationally invariant translation in its most general form

$$\boldsymbol{\mathcal{T}} = -3t_h \boldsymbol{\Lambda}_h + 2t_s \boldsymbol{\Lambda}_s - 2t_a \boldsymbol{\Lambda}_a, \tag{3.32}$$

where the constant parameters t_h, t_s and t_a remain to be found and $\boldsymbol{\Lambda}_a$ is the projector onto the subspace of antisymmetric matrices, the elements of this matrix being given by

$$\{\boldsymbol{\Lambda}_a\}_{ijkl} = \frac{1}{2} \left(\delta_{ik}\delta_{jl} - \delta_{il}\delta_{jk} \right). \tag{3.33}$$

The quasiconvexity test implies that the quadratic form (3.11) must be nonnegative. Since the Fourier components of the displacement gradient matrix are (aside from a factor of i) given by $\hat{\boldsymbol{\zeta}} = \boldsymbol{k} \otimes \hat{\boldsymbol{u}}$, substitution of (3.32) into (3.11) yields

$$\hat{\boldsymbol{\zeta}} \cdot \boldsymbol{\mathcal{T}}\, \hat{\boldsymbol{\zeta}} = (\boldsymbol{k} \otimes \hat{\boldsymbol{u}}) \cdot \boldsymbol{\mathcal{T}}\, (\boldsymbol{k} \otimes \hat{\boldsymbol{u}}) = (t_s - t_a)|\boldsymbol{k}|^2 |\hat{\boldsymbol{u}}|^2 + (-t_h + t_s/3 + t_a)(\boldsymbol{k} \cdot \hat{\boldsymbol{u}})^2 \geq 0, \quad (3.34)$$

which must be nonnegative for any choice of vectors $\boldsymbol{k}$ and $\hat{\boldsymbol{u}}$. This is most easily ensured if we choose

$$t_a = t_s = 3t_h/4 \quad (3.35)$$

so the above expression vanishes for all $\boldsymbol{k}$ and $\hat{\boldsymbol{u}}$, in which case the translation is called a Null-Lagrangian. With this parameter choice the local constraints (3.19) reduce to the set of inequalities

$$\kappa_i + t_h \geq 0, \quad \mu_i - 3t_h/4 \geq 0, \quad t_h \geq 0. \quad (3.36)$$

The bound is obtained from (3.31) which reduces to $y_\kappa \geq t_h$. To find the most restrictive bound one should substitute the maximum permissible value of t_h which in view of the constraints is given by

$$t_h = \frac{4}{3} \min_i \{\mu_i\}. \quad (3.37)$$

Then the bound on the bulk component of the Y-tensor is $y_\kappa \geq \frac{4}{3} \min_i\{\mu_i\}$. By substituting this into (3.27) one can easily see that the bound corresponds to the lower Hashin–Shtrikman bound on the effective bulk modulus of a two-phase composite. The Hashin–Shtrikman upper bound on the effective bulk modulus is associated with minimization of the functional (3.7) which is quadratic in the stress. To obtain it one translates the compliance tensor rather than the stiffness tensor.

4 Coupled bounds

Consider a composite formed from two linear elastic phases with elasticity tensors $\boldsymbol{\mathcal{C}}_i^A$, $i = 1, 2$ and suppose that the effective elastic tensor is $\boldsymbol{\mathcal{C}}_*^A$. Now while retaining the same microgeometry replace the phase materials with new materials with elasticity tensors $\boldsymbol{\mathcal{C}}_i^B$ and let the associated effective tensor be $\boldsymbol{\mathcal{C}}_*^B$.

Following Cherkaev and Gibiansky (1993), in order to obtain correlated bounds for the effective bulk moduli of the composite at states A and B one should consider the following four linear combinations of the functionals above:

$$I_{\tau\tau} \equiv W_\tau^A + W_\tau^B, \tag{4.1}$$
$$I_{\zeta\zeta} \equiv W_\zeta^A + W_\zeta^B, \tag{4.2}$$
$$I_{\tau\zeta} \equiv W_\tau^A + W_\zeta^B, \tag{4.3}$$
$$I_{\zeta\tau} \equiv W_\zeta^A + W_\tau^B, \tag{4.4}$$

where the the superscripts A and B correspond to the energies evaluated at A and B states, respectively. In other words one should find lower bounds on the minimums (as the microstructure is varied) of sums of energies and complementary energies. It has been proved (Francfort and Milton, 1994; Milton, 1994; Milton and Cherkaev, 1995) that knowledge of such minimums suffice to characterize the set of all possible pairs of tensors $(\boldsymbol{\mathcal{C}}_*^A, \boldsymbol{\mathcal{C}}_*^B)$ in a similar way that Legendre transforms characterize convex sets. [In general one needs to consider sums involving more than two energies or complementary energies, but for the coupled bulk modulus bounds sums of two energies should suffice.]

We will show that for the well ordered case the coupled bounds are obtained by considering functionals (4.1) and (4.2), while (4.3) and (4.4) provide the bounds for the badly ordered one. Any of the functionals (4.1)-(4.4) can be represented as a quadratic form by embedding the tensors in ones of a larger dimension

$$I = \boldsymbol{e}_0 \cdot \boldsymbol{\mathcal{L}}_* \, \boldsymbol{e}_0 = \inf_{\langle \boldsymbol{e} \rangle = \boldsymbol{e}_0} \langle \boldsymbol{e}(\boldsymbol{x}) \cdot \boldsymbol{\mathcal{L}}(\boldsymbol{x}) \, \boldsymbol{e}(\boldsymbol{x}) \rangle, \tag{4.5}$$

where $\boldsymbol{e}$ is a vector composed of the tensors of either gradients $\boldsymbol{\zeta}$ or stresses $\boldsymbol{\tau}$ at states A and B. The tensor $\boldsymbol{\mathcal{L}}$ is a block diagonal matrix composed of either stiffness of compliance tensors at states A and B. For example, the functional $I_{\tau\tau}$ can be reexpressed in the form

$$\begin{aligned} I_{\tau\tau} &= \begin{pmatrix} \boldsymbol{\tau}_0^A \\ \boldsymbol{\tau}_0^B \end{pmatrix} \cdot \begin{pmatrix} \boldsymbol{\mathcal{S}}_*^A & 0 \\ 0 & \boldsymbol{\mathcal{S}}_*^B \end{pmatrix} \begin{pmatrix} \boldsymbol{\tau}_0^A \\ \boldsymbol{\tau}_0^B \end{pmatrix} \\ &= \inf_{\substack{\langle \boldsymbol{\tau}^A \rangle = \boldsymbol{\tau}_0^A, \; \langle \boldsymbol{\tau}^B \rangle = \boldsymbol{\tau}_0^B, \\ \nabla \cdot \boldsymbol{\tau}^A = 0, \; \nabla \cdot \boldsymbol{\tau}^B = 0}} \left\langle \begin{pmatrix} \boldsymbol{\tau}^A(\boldsymbol{x}) \\ \boldsymbol{\tau}^B(\boldsymbol{x}) \end{pmatrix} \cdot \begin{pmatrix} \boldsymbol{\mathcal{S}}^A(\boldsymbol{x}) & 0 \\ 0 & \boldsymbol{\mathcal{S}}^B(\boldsymbol{x}) \end{pmatrix} \begin{pmatrix} \boldsymbol{\tau}^A(\boldsymbol{x}) \\ \boldsymbol{\tau}^B(\boldsymbol{x}) \end{pmatrix} \right\rangle, \end{aligned} \tag{4.6}$$

where for generality we do not require that $\boldsymbol{\tau}_0^A = \boldsymbol{\tau}_0^B$. In the formulation (4.5) the fields $\boldsymbol{e}$ must satisfy the appropriate differential constraints, namely $\nabla \cdot \boldsymbol{\tau} = 0$ and $\boldsymbol{\zeta} = \nabla \boldsymbol{u}$.

One is now looking for quasiconvex matrices $\boldsymbol{\mathcal{T}}$ that satisfy constraints (3.15) which become

$$\boldsymbol{\mathcal{L}}_i - \boldsymbol{\mathcal{T}} \geq 0, \quad \forall \;\; i. \tag{4.7}$$

The bounds on the Y-tensor associated with minimization of the functional are given by

$$\boldsymbol{\mathcal{Y}}_* + \boldsymbol{\mathcal{T}} \geq 0, \tag{4.8}$$

where the Y-transformation is defined for the embedded problem by

$$\boldsymbol{\mathcal{Y}}_* = -f_1\boldsymbol{\mathcal{L}}_2 - f_2\boldsymbol{\mathcal{L}}_1 - f_1f_2(\boldsymbol{\mathcal{L}}_1 - \boldsymbol{\mathcal{L}}_2)(\boldsymbol{\mathcal{L}}_* - f_1\boldsymbol{\mathcal{L}}_1 - f_2\boldsymbol{\mathcal{L}}_2)^{-1}(\boldsymbol{\mathcal{L}}_1 - \boldsymbol{\mathcal{L}}_2). \tag{4.9}$$

The matrix $\boldsymbol{\mathcal{T}}$ should be chosen to make the bounds the most restrictive.

4.1 The badly ordered case

4.1.1 Lower Bound

We restrict ourselves to the case when two isotropic viscoelastic materials are mixed together to form an isotropic composite. For isotropic phases the stiffness tensors $\boldsymbol{\mathcal{C}}_i^{A,B}$ at states A or B can be decomposed into a hydrostatic part characterized by the bulk modulus and a trace-free part characterized by the shear modulus:

$$\boldsymbol{\mathcal{C}}_i^{A,B} = 3\kappa_i^{A,B}\boldsymbol{\Lambda}_h + 2\mu_i^{A,B}\boldsymbol{\Lambda}_s.$$

This is also applicable to the effective stiffness tensor of an isotropic composite:

$$\boldsymbol{\mathcal{C}}_*^{A,B} = 3\kappa_*^{A,B}\boldsymbol{\Lambda}_h + 2\mu_*^{A,B}\boldsymbol{\Lambda}_s,$$

where κ_* and μ_* are the effective bulk and shear moduli of the composite, respectively. Consequently, the isotropic fourth-order tensor $\boldsymbol{\mathcal{Y}}_*$ has a similar decomposition:

$$\boldsymbol{\mathcal{Y}}_*^{A,B} = 3y_\kappa^{A,B}\boldsymbol{\Lambda}_h + 2y_\mu^{A,B}\boldsymbol{\Lambda}_s$$

where

$$\begin{aligned} y_\kappa = & \quad -f_2\kappa_1 - f_1\kappa_2 - \frac{f_1f_2(\kappa_1-\kappa_2)^2}{\kappa_* - f_1\kappa_1 - f_2\kappa_2}, \\ y_\mu = & \quad -f_2\mu_1 - f_1\mu_2 - \frac{f_1f_2(\mu_1-\mu_2)^2}{\mu_* - f_1\mu_1 - f_2\mu_2}. \end{aligned} \tag{4.10}$$

Here the superscripts A and B are omitted for simplicity of the expressions and should be added to all elastic moduli in an appropriate place.

Let us consider the badly ordered case first. The constitutive relations for the states A and B of the composite media are described by the equations

$$\begin{aligned} \boldsymbol{\tau}^A(\boldsymbol{x}) &= \left(3\kappa^A(\boldsymbol{x})\boldsymbol{\Lambda}_h + 2\mu^A(\boldsymbol{x})\boldsymbol{\Lambda}_s\right)\boldsymbol{\zeta}^A(\boldsymbol{x}), \\ \boldsymbol{\tau}^B(\boldsymbol{x}) &= \left(3\kappa^B(\boldsymbol{x})\boldsymbol{\Lambda}_h + 2\mu^B(\boldsymbol{x})\boldsymbol{\Lambda}_s\right)\boldsymbol{\zeta}^B(\boldsymbol{x}). \end{aligned} \tag{4.11}$$

We embed the equations into a larger problem where the constitutive relations take the form

$$\begin{pmatrix} \boldsymbol{\tau}^A(\boldsymbol{x}) \\ \boldsymbol{\tau}^B(\boldsymbol{x}) \end{pmatrix} = \boldsymbol{\mathcal{L}}(\boldsymbol{x}) \begin{pmatrix} \boldsymbol{\zeta}^A(\boldsymbol{x}) \\ \boldsymbol{\zeta}^B(\boldsymbol{x}) \end{pmatrix}, \tag{4.12}$$

in which

$$\boldsymbol{\mathcal{L}}(\boldsymbol{x}) = \left(\boldsymbol{\mathcal{L}}_1\chi_1(\boldsymbol{x}) + \boldsymbol{\mathcal{L}}_2\chi_2(\boldsymbol{x})\right), \tag{4.13}$$

and $\chi_i(\boldsymbol{x})$ indicates whether the point $\boldsymbol{x}$ lies in the domain occupied by phase i:

$$\chi_i(\boldsymbol{x}) = \begin{cases} 1, & \text{if } \boldsymbol{x} \in \Omega_i \\ 0, & \text{otherwise.} \end{cases} \tag{4.14}$$

and the $\boldsymbol{\mathcal{L}}_i$ are defined as

$$\boldsymbol{\mathcal{L}}_i = \begin{pmatrix} 3\kappa_i^A\boldsymbol{\Lambda}_h + 2\mu_i^A\boldsymbol{\Lambda}_s & 0 \\ 0 & 3\kappa_i^B\boldsymbol{\Lambda}_h + 2\mu_i^B\boldsymbol{\Lambda}_s \end{pmatrix}. \tag{4.15}$$

The associated $\boldsymbol{\mathcal{Y}}_*$ tensor then is

$$\boldsymbol{\mathcal{Y}}_* = \begin{pmatrix} 3y_\kappa^A\boldsymbol{\Lambda}_h + 2y_\mu^A\boldsymbol{\Lambda}_s & 0 \\ 0 & 3y_\kappa^B\boldsymbol{\Lambda}_h + 2y_\mu^B\boldsymbol{\Lambda}_s \end{pmatrix}. \tag{4.16}$$

The current problem is similar in many respects to the problem of coupling the effective bulk modulus and effective conductivity of a composite, for which Gibiansky and Torquato (1996a) used the translation method to improve the bounds of Berryman and Milton (1988) [see also the recent paper of Nesi and Rogora (2004), who treat the coupling of two conductivity problems using the translation method]. The translation tensor $\boldsymbol{\mathcal{T}}$ can be taken as the following Null-Lagrangian

$$\boldsymbol{\mathcal{T}} = \begin{pmatrix} -t_1(2\boldsymbol{\Lambda}_h - \boldsymbol{\Lambda}_s + \boldsymbol{\Lambda}_a) & -t_3(2\boldsymbol{\Lambda}_h - \boldsymbol{\Lambda}_s + \boldsymbol{\Lambda}_a) \\ -t_3(2\boldsymbol{\Lambda}_h - \boldsymbol{\Lambda}_s + \boldsymbol{\Lambda}_a) & -t_2(2\boldsymbol{\Lambda}_h - \boldsymbol{\Lambda}_s + \boldsymbol{\Lambda}_a) \end{pmatrix}. \tag{4.17}$$

Since the projections $\boldsymbol{\Lambda}_h$, $\boldsymbol{\Lambda}_s$ and $\boldsymbol{\Lambda}_a$ project onto orthogonal subspaces the constraint $\boldsymbol{\mathcal{L}}_i - \boldsymbol{\mathcal{T}} \geq 0$, which for the present case has the form

$$\boldsymbol{\mathcal{L}}_i - \boldsymbol{\mathcal{T}} = \begin{pmatrix} (3\kappa_i^A + 2t_1)\boldsymbol{\Lambda}_h + (2\mu_i^A - t_1)\boldsymbol{\Lambda}_s + t_1\boldsymbol{\Lambda}_a & t_3(2\boldsymbol{\Lambda}_h - \boldsymbol{\Lambda}_s + \boldsymbol{\Lambda}_a) \\ -t_3(2\boldsymbol{\Lambda}_h - \boldsymbol{\Lambda}_s + \boldsymbol{\Lambda}_a) & (3\kappa_i^B + 2t_2)\boldsymbol{\Lambda}_h + (2\mu_i^B - t_2)\boldsymbol{\Lambda}_s + t_2\boldsymbol{\Lambda}_a \end{pmatrix}, \tag{4.18}$$

can be decomposed into a set of constraints:

$$\begin{pmatrix} 3\kappa_i^A + 2t_1 & 2t_3 \\ 2t_3 & 3\kappa_i^B + 2t_2 \end{pmatrix} \geq 0, \quad \begin{pmatrix} 2\mu_i^A - t_1 & -t_3 \\ -t_3 & 2\mu_i^B - t_2 \end{pmatrix} \geq 0, \quad \begin{pmatrix} t_1 & t_3 \\ t_3 & t_2 \end{pmatrix} \geq 0. \quad (4.19)$$

These equations are satisfied if the leading elements of the matrices and their determinants are nonnegative. The last equation requires that $t_1 \geq 0$ and $t_1 t_2 \geq t_3^2$. The second equation leads us to the conclusion that $t_1 \leq \min_i \{2\mu_i^A\}$. It also follows that the parameters t_1, t_2 and t_3 must be chosen such that the inequality

$$\left(\frac{3}{2}y_1 - t_1\right)\left(\frac{3}{2}y_2 - t_2\right) - t_3^2 \geq 0, \quad (4.20)$$

is valid for the following five points (y_1, y_2) in the $y_\kappa^A - y_\kappa^B$ plane:

$$(0,0), \quad (-\kappa_i^A, -\kappa_i^B), \quad (\frac{4}{3}\mu_i^A, \frac{4}{3}\mu_i^B), \quad i = 1,2. \quad (4.21)$$

The inequality $\boldsymbol{\mathcal{Y}}_* + \boldsymbol{\mathcal{T}} \geq 0$ that provides the bounds on the Y-tensor assumes the form

$$\begin{pmatrix} 3y_\kappa^A - 2t_1 & -2t_3 \\ -2t_3 & 3y_\kappa^B - 2t_2 \end{pmatrix} \geq 0. \quad (4.22)$$

By comparing the determinant of this matrix to (4.20) we conclude that the point (y_κ^A, y_κ^B) lies in the region defined by (4.20).

The positivity of t_1 implies that the vertical asymptote of the hyperbola (4.20) lies in the right half of the plane. This will be satisfied if the points $(-\kappa_i^A, -\kappa_i^B), i = 1,2,$ and the origin of the plane lie below the lower branch of the hyperbola. Similarly the restriction that $t_1 \leq \min_i\{2\mu_i^A\}$ will be satisfied if the points $(\frac{4}{3}\mu_i^A, \frac{4}{3}\mu_i^B)$, $i = 1,2$, lie above the upper branch of the hyperbola,

One can now move and resize the hyperbola (4.20) to get the most restrictive bounds, which in fact corresponds to moving the branches of the hyperbola as far apart as possible. It must be done so that the two points $(\frac{4}{3}\mu_i^A, \frac{4}{3}\mu_i^B)$, $i = 1,2$, lie above the upper branch of the hyperbola, while the two points $(-\kappa_i^A, -\kappa_i^B), i = 1,2,$ and the origin of the plane lie below the lower branch. Keeping in mind that

$$(\mu_2^A - \mu_1^A)(\mu_2^B - \mu_1^B) < 0, \quad (4.23)$$

we can see that the best bounds are obtained when the upper branch of the hyperbola passes through the points $(\frac{4}{3}\mu_i^A, \frac{4}{3}\mu_i^B)$ and the lower branch intersects the origin (see Figure 6). It easy to show that this corresponds to the following expressions for the

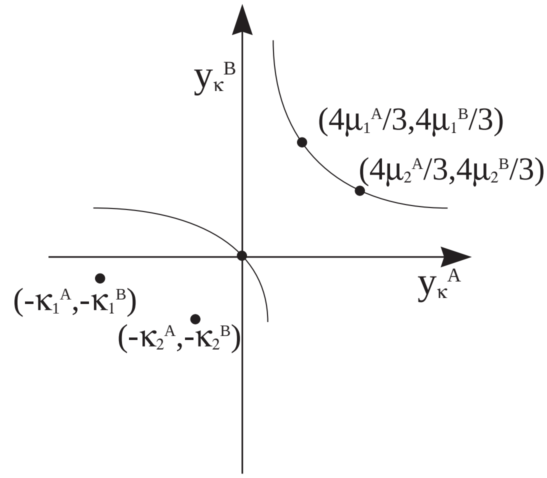

Fig. 6. Schematic representation of the optimal hyperbola in the (y_κ^A, y_κ^B) plane which leads to the lower bound in the badly ordered case. The hyperbola passes through the points in the first quadrant that correspond to the Hashin–Shtrikman bounds and the origin of the coordinate system.

parameters t_1, t_2 and t_3

$$t_1 = 2\frac{\mu_1^A \mu_2^A (\mu_2^B - \mu_1^B)}{\mu_1^A \mu_2^B - \mu_2^A \mu_1^B}, \quad t_2 = -2\frac{\mu_1^B \mu_2^B (\mu_2^A - \mu_1^A)}{\mu_1^A \mu_2^B - \mu_2^A \mu_1^B}, \quad t_3^2 = t_1 t_2, \tag{4.24}$$

and consequently the bound (4.20) with $(y_1, y_2) = (y_\kappa^A, y_\kappa^B)$ reduces to the bound (2.5). Notice that the points $(y_\kappa^A, y_\kappa^B) = (\frac{4}{3}\mu_i^A, \frac{4}{3}\mu_i^B)$ correspond to the Hashin–Shtrikman bounds.

4.1.2 Upper Bound

Let us now derive the bound on the Y-tensor that is associated with the functional $I_{\zeta\zeta}$ which is quadratic in the stresses. The constitutive relations are

$$\begin{aligned} \boldsymbol{\varepsilon}^A(\boldsymbol{x}) &= \left(\frac{1}{3\kappa^A(\boldsymbol{x})} \boldsymbol{\Lambda}_h + \frac{1}{2\mu^A(\boldsymbol{x})} \boldsymbol{\Lambda}_s \right) \boldsymbol{\tau}^A(\boldsymbol{x}), \\ \boldsymbol{\varepsilon}^B(\boldsymbol{x}) &= \left(\frac{1}{3\kappa^B(\boldsymbol{x})} \boldsymbol{\Lambda}_h + \frac{1}{2\mu^B(\boldsymbol{x})} \boldsymbol{\Lambda}_s \right) \boldsymbol{\tau}^B(\boldsymbol{x}). \end{aligned} \tag{4.25}$$

Embedding these into a problem of larger dimension, we consider a new quadratic form

$$\begin{pmatrix} \boldsymbol{\tau}^A(\boldsymbol{x}) \\ \boldsymbol{\tau}^B(\boldsymbol{x}) \end{pmatrix}^T \boldsymbol{\mathcal{L}}(\boldsymbol{x}) \begin{pmatrix} \boldsymbol{\tau}^A(\boldsymbol{x}) \\ \boldsymbol{\tau}^B(\boldsymbol{x}) \end{pmatrix}, \tag{4.26}$$

where $\boldsymbol{\mathcal{L}}(\boldsymbol{x})$ is defined as in the previous case by (4.13) and

$$\boldsymbol{\mathcal{L}}_i = \begin{pmatrix} \frac{1}{3\kappa_i^A}\boldsymbol{\Lambda}_h + \frac{1}{2\mu_i^A}\boldsymbol{\Lambda}_s & 0 \\ 0 & \frac{1}{3\kappa_i^B}\boldsymbol{\Lambda}_h + \frac{1}{2\mu_i^B}\boldsymbol{\Lambda}_s \end{pmatrix}. \tag{4.27}$$

The corresponding Y-tensor has the form

$$\boldsymbol{\mathcal{Y}}_* = \begin{pmatrix} \frac{1}{3y_\kappa^A}\boldsymbol{\Lambda}_h + \frac{1}{2y_\mu^A}\boldsymbol{\Lambda}_s & 0 \\ 0 & \frac{1}{3y_\kappa^B}\boldsymbol{\Lambda}_h + \frac{1}{2y_\mu^B}\boldsymbol{\Lambda}_s \end{pmatrix}. \tag{4.28}$$

Here the following essential feature of the Y-transformation is used (see, for example, Milton, 2002)

$$\boldsymbol{\mathcal{Y}}_*(\boldsymbol{\mathcal{L}}_i^{-1}, \boldsymbol{\mathcal{L}}_*^{-1}, f_i) = \boldsymbol{\mathcal{Y}}_*^{-1}(\boldsymbol{\mathcal{L}}_i, \boldsymbol{\mathcal{L}}_*, f_i). \tag{4.29}$$

We take a translation matrix $\boldsymbol{\mathcal{T}}$ with a similar isotropic form

$$\boldsymbol{\mathcal{T}} = \begin{pmatrix} t_1\boldsymbol{\Lambda}_h + t_2\boldsymbol{\Lambda}_s & t_3\boldsymbol{\Lambda}_h + t_4\boldsymbol{\Lambda}_s \\ t_3\boldsymbol{\Lambda}_h + t_4\boldsymbol{\Lambda}_s & t_5\boldsymbol{\Lambda}_h + t_6\boldsymbol{\Lambda}_s \end{pmatrix}, \tag{4.30}$$

where the constant coefficients $t_1 - t_6$ remain to be chosen. There is no point in including $\boldsymbol{\Lambda}_a$ in the blocks of the translation because it does not influence the quadratic form, since it vanishes after being multiplied twice by a symmetric second-order stress tensor.

Now let us apply the quasiconvexity test. The differential constraints on the stress in Fourier space have the form

$$\boldsymbol{k} \cdot \hat{\boldsymbol{\tau}} = 0, \tag{4.31}$$

where $\boldsymbol{k}$ is the wavevector. So $\boldsymbol{\mathcal{T}}$ will be quasiconvex if for all $\boldsymbol{k}$

$$\begin{pmatrix} \boldsymbol{\tau}^A \\ \boldsymbol{\tau}^B \end{pmatrix} \cdot \begin{pmatrix} t_1\boldsymbol{\Lambda}_h + t_2\boldsymbol{\Lambda}_s & t_3\boldsymbol{\Lambda}_h + t_4\boldsymbol{\Lambda}_s \\ t_3\boldsymbol{\Lambda}_h + t_4\boldsymbol{\Lambda}_s & t_5\boldsymbol{\Lambda}_h + t_6\boldsymbol{\Lambda}_s \end{pmatrix} \begin{pmatrix} \boldsymbol{\tau}^A \\ \boldsymbol{\tau}^B \end{pmatrix} \geq 0, \tag{4.32}$$

for all $\boldsymbol{\tau}^A$ and $\boldsymbol{\tau}^B$ with $\boldsymbol{k} \cdot \boldsymbol{\tau}^A = \boldsymbol{k} \cdot \boldsymbol{\tau}^B = 0$. Because of the rotational invariance of $\boldsymbol{\mathcal{T}}$ it suffices to check the inequality for $k = \{1, 0, 0\}$. In this case (4.31) implies the Fourier transform of the stress tensor has the form

$$\hat{\boldsymbol{\tau}} = \begin{pmatrix} 0 & 0 & 0 \\ 0 & \hat{\tau}_{22} & \hat{\tau}_{23} \\ 0 & \hat{\tau}_{23} & \hat{\tau}_{33} \end{pmatrix}. \tag{4.33}$$

By substituting (4.33) into (4.32) and performing straightforward algebraic manipulation, one can show that the following quadratic form is required to be nonnegative to ensure the quasiconvexity of the translation $\boldsymbol{\mathcal{T}}$

$$\begin{pmatrix} \hat{\tau}^A_{22}+\tau^A_{33} \\ \hat{\tau}^B_{22}+\tau^B_{33} \\ \hat{\tau}^A_{22}-\tau^A_{33} \\ \hat{\tau}^B_{22}-\tau^B_{33} \\ \hat{\tau}^A_{23} \\ \hat{\tau}^B_{23} \end{pmatrix} \cdot \begin{pmatrix} \frac{1}{3}(2t_1+t_2) & \frac{1}{3}(2t_3+t_4) & 0 & 0 & 0 & 0 \\ \frac{1}{3}(2t_3+t_4) & \frac{1}{3}(2t_5+t_6) & 0 & 0 & 0 & 0 \\ 0 & 0 & t_2 & t_4 & 0 & 0 \\ 0 & 0 & t_4 & t_6 & 0 & 0 \\ 0 & 0 & 0 & 0 & 2t_2 & 2t_4 \\ 0 & 0 & 0 & 0 & 2t_4 & 2t_6 \end{pmatrix} \begin{pmatrix} \hat{\tau}^A_{22}+\tau^A_{33} \\ \hat{\tau}^B_{22}+\tau^B_{33} \\ \hat{\tau}^A_{22}-\tau^A_{33} \\ \hat{\tau}^B_{22}-\tau^B_{33} \\ \hat{\tau}^A_{23} \\ \hat{\tau}^B_{23} \end{pmatrix} \geq 0. \tag{4.34}$$

The block-diagonal matrix appearing in this quadratic form will clearly be positive semidefinite provided its blocks are positive semidefinite, i.e., provided that the matrix elements satisfy the following set of inequalities

$$t_2 \geq 0, \quad 2t_1+t_2 \geq 0, \quad t_2t_6-t_4^2 \geq 0 \quad (2t_1+t_2)(2t_5+t_6)-(2t_3+t_4)^2 \geq 0. \tag{4.35}$$

Next we consider the inequalities (4.7) and (4.8) which after substitution of (4.27), (4.28) and (4.30) reduce to the set of constraints

$$\begin{pmatrix} 1/3\kappa_i^A - t_1 & -t_3 \\ -t_3 & 1/3\kappa_i^B - t_5 \end{pmatrix} \geq 0, \quad \begin{pmatrix} 1/2\mu_i^A - t_2 & -t_4 \\ -t_4 & 1/2\mu_i^B - t_6 \end{pmatrix} \geq 0, \tag{4.36}$$

and to the following bounds on y_κ

$$\begin{pmatrix} 1/3y_\kappa^A + t_1 & t_3 \\ t_3 & 1/3y_\kappa^B + t_5 \end{pmatrix} \geq 0. \tag{4.37}$$

Obtaining the best bounds requires optimization over the six unknown parameters t_1–t_6 taking into account the numerous constraints, which is a quite difficult task. To simplify the problem (at the possible cost of getting suboptimal bounds) it seems natural to choose these six parameters so that the matrix appearing in (4.34) is highly degenerate. There are various ways to do this. One choice, which results in useful bounds, is to require that the first block in the matrix vanish, i.e. that

$$2t_1+t_2=0, \quad 2t_5+t_6=0, \quad 2t_3+t_4=0, \tag{4.38}$$

which ensures that the matrix has at most rank 4. After this simplification the inequalities become

$$\begin{pmatrix} 2/3\kappa_i^A + t_2 & t_4 \\ t_4 & 2/3\kappa_i^B + t_6 \end{pmatrix} \geq 0, \quad \begin{pmatrix} 1/2\mu_i^A - t_2 & -t_4 \\ -t_4 & 1/2\mu_i^B - t_6 \end{pmatrix} \geq 0, \tag{4.39}$$

$$\begin{pmatrix} 2/3y_\kappa^A - t_2 & -t_4 \\ -t_4 & 2/3y_\kappa^B - t_6 \end{pmatrix} \geq 0. \tag{4.40}$$

Since the determinant of the latter matrix is nonnegative, we can consider a hyperbola in the $(1/y_\kappa^A, 1/y_\kappa^B)$ plane that defines the bounds on the y-parameters

$$\left(\frac{2}{3}\frac{1}{y_\kappa^A} - t_2\right)\left(\frac{2}{3}\frac{1}{y_\kappa^B} - t_6\right) - t_4^2 \geq 0. \tag{4.41}$$

From the inequalities (4.39) it can be immediately concluded that the parameter t_2 must obey $0 \leq t_2 \leq \min_i\{1/2\mu_i^A\}$. This constrains the position of the vertical asymptote of the hyperbola, and it then follows from (4.39) that the points $(-1/k_i^A, -1/k_i^B)$ must lie below the lower branch of the hyperbola, while the points $(3/4\mu_i^A, 3/4\mu_i^B)$ must lie above the upper branch of the hyperbola. One also realizes that the nonnegativity of the lower-right block in the matrix appearing in (4.34)

$$\begin{pmatrix} t_2 & t_4 \\ t_4 & t_6 \end{pmatrix} \geq 0,$$

requires that the origin of the coordinate system lies under the lower branch of the hyperbola. Similar to the previous case we move and resize the hyperbola while trying to locate the branches as far apart as possible, keeping in mind that the case under consideration is the badly ordered one. Doing this, we find that the lower branch of the hyperbola must cross the origin of the coordinate system and the upper branch passes through the two points $(3/4\mu_i^A, 3/4\mu_i^B)$, see Figure 7. It follows that $t_2 t_6 = t_4^2$ (which implies the the matrix appearing in (4.34) has at most rank 2) and by taking the determinant of the second set of inequalities in (4.39) we obtain a system of two equalities, which is to be solved for the parameters t_2 and t_6. The solution of these algebraic equations takes the form

$$t_2 = \frac{1}{2}\frac{\mu_1^B - \mu_2^B}{\mu_1^B\mu_2^A - \mu_1^A\mu_2^B}, \quad t_6 = -\frac{1}{2}\frac{\mu_1^A - \mu_2^A}{\mu_1^B\mu_2^A - \mu_1^A\mu_2^B}. \tag{4.42}$$

Similar to the previous case the constraints for the points $(-\kappa_i^A, -\kappa_i^B)$ are automatically satisfied, since the lower branch of the hyperbola does not cross the third quadrant. We also note that the points $(3/4\mu_i^A, 3/4\mu_i^B), i = 1, 2$ through which the upper branch of the hyperbola passes correspond to the Hashin–Shtrikman bounds.

The inequality (4.41) can be simplified by using the relation $t_2 t_6 = t_4^2$ and reduces to the equation of a straight line in the (y_κ^A, y_κ^B) plane connecting the two Hashin–Shtrikman points $(3/4\mu_i^A, 3/4\mu_i^B)$:

$$\frac{3}{2}t_2 y_\kappa^A + \frac{3}{2}t_6 y_\kappa^B \leq 1, \tag{4.43}$$

which is equivalent to (2.4).

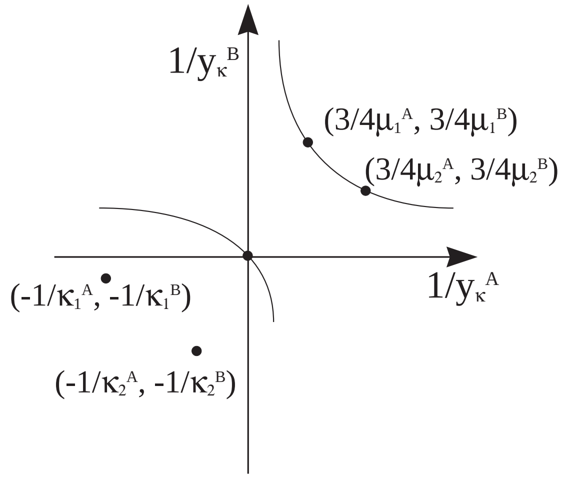

Fig. 7. Schematic representation of the optimal hyperbola in the $(1/y_\kappa^A, 1/y_\kappa^B)$ plane which leads to the upper bound in the badly ordered case. The hyperbola passes through the points in the first quadrant that correspond to the Hashin–Shtrikman bounds and the origin of the coordinate system.

The correlated bounds in the badly ordered case can be used to recover the phase-interchange bounds by Gibiansky and Torquato (1996b) who implemented the geometrical-parameter method of Milton and Phan-Thien (1982) and Berryman and Milton (1988) to derive their bounds. Assume that the effective bulk modulus of a two-phase linear elastic composite κ_*^A is known and ask what can be said about the effective bulk modulus κ_*^B of a composite with interchanged phases. Switching phases implies the following substitution:

$$\mu_2^B = \mu_1^A = \mu_1, \quad \mu_2^A = \mu_1^B = \mu_2, \tag{4.44}$$

which satisfies the condition for the badly ordered case. Then the lower bound on y_κ^B defined by (2.5) reduces to

$$y_\kappa^A + y_\kappa^B \leq \frac{4}{3}(\mu_1 + \mu_2), \tag{4.45}$$

while the upper bound (2.6) assumes the form

$$\frac{1}{y_\kappa^A} + \frac{1}{y_\kappa^B} \leq \frac{3}{4}\left(\frac{1}{\mu_1} + \frac{1}{\mu_2}\right), \tag{4.46}$$

which are precisely the bounds of Gibiansky and Torquato (1996b). Notice that although the relations (4.44) do not have a physical meaning in the viscoelastic case, where the moduli obey the inequalities $\mu_i^B < \mu_i^A$, $i = 1, 2$, the formulation of our problem is such that these inequalities are not used in the derivation of the coupled bounds: they apply to any pair of elastic composites sharing the same microstructure.

4.2.1 First mixed bound

In order to obtain the bounds in the well ordered case we consider the functionals $I_{\zeta\tau}$ and $I_{\tau\zeta}$ that combine the strain and stress energies stored in the composite at states A and B. Since the treatment of the bounds on the Y-tensor associated with each functional is virtually identical, we only derive the bounds associated with minimization of $I_{\tau\zeta}$: the derivation of the bounds associated with minimization of the functional $I_{\zeta\tau}$ merely requires switching the properties A and B.

We will see that the bounds associated with the minimization of $I_{\tau\zeta}$, provide an upper bound on y_κ^A for fixed y_κ^B but a lower bound on y_κ^B for fixed y_κ^A. Thus they are best described as mixed bounds on the moduli. The constitutive relations for the fields to be used with the functional $I_{\tau\zeta}$ assume the form

$$\begin{aligned}
\boldsymbol{\zeta}^A(\boldsymbol{x}) &= \left(\frac{1}{3\kappa^A(\boldsymbol{x})}\boldsymbol{\Lambda}_h + \frac{1}{2\mu^A(\boldsymbol{x})}\boldsymbol{\Lambda}_s\right)\boldsymbol{\tau}^A(\boldsymbol{x}),\\
\boldsymbol{\tau}^B(\boldsymbol{x}) &= \left(3\kappa^B(\boldsymbol{x})\boldsymbol{\Lambda}_h + 2\mu^B(\boldsymbol{x})\boldsymbol{\Lambda}_s\right)\boldsymbol{\zeta}^B(\boldsymbol{x}).
\end{aligned} \tag{4.47}$$

The quadratic form of the local energy is written as follows

$$I_{\tau\zeta} = \begin{pmatrix}\boldsymbol{\tau}^A(\boldsymbol{x})\\ \boldsymbol{\zeta}^B(\boldsymbol{x})\end{pmatrix}\cdot\boldsymbol{\mathcal{L}}(\boldsymbol{x})\begin{pmatrix}\boldsymbol{\tau}^A(\boldsymbol{x})\\ \boldsymbol{\zeta}^B(\boldsymbol{x})\end{pmatrix}, \tag{4.48}$$

where $\boldsymbol{\mathcal{L}}(\boldsymbol{x}) = \sum_{i=1}^{2}\boldsymbol{\mathcal{L}}_i\chi_i(x)$ and the $\boldsymbol{\mathcal{L}}_i$ are defined by

$$\boldsymbol{\mathcal{L}}_i = \begin{pmatrix}\frac{1}{3\kappa_i^A}\boldsymbol{\Lambda}_h + \frac{1}{2\mu_i^A}\boldsymbol{\Lambda}_s & 0\\ 0 & 3\kappa_i^B\boldsymbol{\Lambda}_h + 2\mu_i^B\boldsymbol{\Lambda}_s\end{pmatrix}. \tag{4.49}$$

The corresponding Y-tensor becomes

$$\boldsymbol{\mathcal{Y}}_* = \begin{pmatrix}\frac{1}{3y_\kappa^A}\boldsymbol{\Lambda}_h + \frac{1}{2y_\mu^A}\boldsymbol{\Lambda}_s & 0\\ 0 & 3y_\kappa^B\boldsymbol{\Lambda}_h + 2y_\mu^B\boldsymbol{\Lambda}_s\end{pmatrix}. \tag{4.50}$$

We take a rotationally invariant translation matrix of the form

$$\boldsymbol{\mathcal{T}} = \begin{pmatrix}t_1\boldsymbol{\Lambda}_h + t_2\boldsymbol{\Lambda}_s & t_3\boldsymbol{\Lambda}_h + t_4\boldsymbol{\Lambda}_s\\ t_3\boldsymbol{\Lambda}_h + t_4\boldsymbol{\Lambda}_s & t_5\boldsymbol{\Lambda}_h + t_6\boldsymbol{\Lambda}_s + t_7\boldsymbol{\Lambda}_a\end{pmatrix}, \tag{4.51}$$

where the antisymmetric part $t_7\mathbf{\Lambda}_a$ is added to the block that undergoes double multiplication by the nonsymmetric matrix $\boldsymbol{\zeta}^B(\boldsymbol{x})$.

Analogously to the previous case the quasiconvexity of $\boldsymbol{\mathcal{T}}$ requires that

$$\begin{pmatrix} \hat{\boldsymbol{\tau}}^A \\ \hat{\boldsymbol{\zeta}}^B \end{pmatrix} \cdot \begin{pmatrix} t_1\mathbf{\Lambda}_h + t_2\mathbf{\Lambda}_s & t_3\mathbf{\Lambda}_h + t_4\mathbf{\Lambda}_s \\ t_3\mathbf{\Lambda}_h + t_4\mathbf{\Lambda}_s & t_5\mathbf{\Lambda}_h + t_6\mathbf{\Lambda}_s + t_7\mathbf{\Lambda}_a \end{pmatrix} \begin{pmatrix} \hat{\boldsymbol{\tau}}^A \\ \hat{\boldsymbol{\zeta}}^B \end{pmatrix} \geq 0, \tag{4.52}$$

where $\hat{\boldsymbol{\tau}}^A(\boldsymbol{k})$ and $\hat{\boldsymbol{\zeta}}^B(\boldsymbol{k})$ are the Fourier components of the stresses at state A and the displacement gradient at state B, respectively. To test the quasiconvexity of the translation matrix we choose the wavevector to be $\boldsymbol{k} = \{1, 0, 0\}$. Then the components of the stress tensor is given by (4.33) and the displacement gradient Fourier component $\hat{\boldsymbol{\zeta}}(\mathbf{k})$ assumes the form

$$\hat{\boldsymbol{\zeta}}(\boldsymbol{k}) = \boldsymbol{k} \otimes \hat{\boldsymbol{u}} = \begin{pmatrix} \hat{u}_1 & \hat{u}_2 & \hat{u}_3 \\ 0 & 0 & 0 \\ 0 & 0 & 0 \end{pmatrix}, \tag{4.53}$$

where the $\hat{u}_i$ are the Fourier components of the displacement vector (aside from a factor of i). Substitution of (4.33) and (4.53) into (4.52) reduces (4.52) to the requirement of nonnegativity of the following quadratic form

$$\begin{pmatrix} \hat{\tau}^A_{22} + \hat{\tau}^A_{33} \\ \hat{u}^B_1 \\ \hat{\tau}^A_{22} - \hat{\tau}^A_{33} \\ \hat{\tau}^A_{23} \\ \hat{u}^B_2 \\ \hat{u}^B_3 \end{pmatrix} \cdot \begin{pmatrix} \frac{1}{6}(2t_1 + t_2) & \frac{1}{3}(t_3 - t_4) & 0 & 0 & 0 & 0 \\ \frac{1}{3}(t_3 - t_4) & \frac{1}{3}(t_5 + 2t_6) & 0 & 0 & 0 & 0 \\ 0 & 0 & t_2 & 0 & 0 & 0 \\ 0 & 0 & 0 & 2t_2 & 0 & 0 \\ 0 & 0 & 0 & 0 & \frac{1}{2}(t_6 + t_7) & 0 \\ 0 & 0 & 0 & 0 & 0 & \frac{1}{2}(t_6 + t_7) \end{pmatrix} \begin{pmatrix} \hat{\tau}^A_{22} + \hat{\tau}^A_{33} \\ \hat{u}^B_1 \\ \hat{\tau}^A_{22} - \hat{\tau}^A_{33} \\ \hat{\tau}^A_{23} \\ \hat{u}^B_2 \\ \hat{u}^B_3 \end{pmatrix} \geq 0. \tag{4.54}$$

For this quadratic form to be positive, the following constraints on the translation parameters must be satisfied

$$t_2 \geq 0, \quad 2t_1 + t_2 \geq 0, \quad t_6 + t_7 \geq 0, \quad (2t_1 + t_2)(t_5 + 2t_6) - 2(t_3 - t_4)^2 \geq 0. \tag{4.55}$$

The inequalities (4.7) after decomposition onto orthogonal subspaces provide the set of constraints

$$\begin{pmatrix} 1/3\kappa^A_i - t_1 & -t_3 \\ -t_3 & 3\kappa^B_i - t_5 \end{pmatrix} \geq 0, \quad \begin{pmatrix} 1/2\mu^A_i - t_2 & -t_4 \\ -t_4 & 2\mu^B_i - t_6 \end{pmatrix} \geq 0, \quad \begin{pmatrix} 0 & 0 \\ 0 & -t_7 \end{pmatrix} \geq 0, \tag{4.56}$$

and the bound (4.8) on y_κ becomes

$$\begin{pmatrix} 1/3y_\kappa^A + t_1 & t_3 \\ t_3 & 3y_\kappa^B + t_5 \end{pmatrix} \geq 0. \tag{4.57}$$

Based on the success of the approach in the badly ordered case it seems natural to choose the seven parameters $t_1 - t_7$ so that the first block of the matrix appearing in (4.34) vanishes, i.e.

$$2t_1 + t_2 = 0, \quad t_5 + 2t_6 = 0 \quad \text{and} \quad t_3 - t_4 = 0. \tag{4.58}$$

Then eliminating t_1, t_3 and t_5 the set of inequalities becomes

$$\begin{pmatrix} 2/3\kappa_i^A + t_2 & t_4 \\ t_4 & 3\kappa_i^B/2 + t_6 \end{pmatrix} \geq 0, \quad \begin{pmatrix} 1/2\mu_i^A - t_2 & -t_4 \\ -t_4 & 2\mu_i^B - t_6 \end{pmatrix} \geq 0, \tag{4.59}$$

$$\begin{pmatrix} 2/3y_\kappa^A - t_2 & -t_4 \\ -t_4 & 3y_\kappa^B/2 - t_6 \end{pmatrix} \geq 0, \tag{4.60}$$

which is quite similar to the form of the inequalities in the previous well-ordered case, except that now the moduli for the A case are replaced by their inverses.

The latter constraint provides an inequality for the coupled bounds

$$\left(\frac{2}{3y_\kappa^A} - t_2\right)\left(\frac{3}{2}y_\kappa^B - t_6\right) - t_4^2 \geq 0, \tag{4.61}$$

which again defines a hyperbola, but contrary to the previous case, in the $(1/y_\kappa^A, y_\kappa^B)$ plane. From the inequalities (4.55), (4.56) and (4.59) is it clear that

$$0 \leq t_2 \leq \min_i\{1/2\mu_i^A\}, \quad \text{and} \quad 0 \leq t_6 \leq \min_i\{2\mu_i^B\}, \tag{4.62}$$

which places constraints on the vertical and horizonal positions of the asymptotes of the hyperbola. Consequently it follows from (4.59) that the points $(-1/\kappa_i^A, -\kappa_i^B)$ lie below the lower branch of the hyperbola and while the points $(3/4\mu_i^A, 4\mu_i^B/3)$ are located above the second branch, which is concave up.

In this case, in an attempt to separate the branches of the hyperbola (4.61) far apart, one should move the asymptotes towards the origin of the coordinate system by decreasing the values of t_2 and t_6. However, since there is no restriction that prescribes the location of the branches with respect to the origin of the coordinate system, the lower branch can partially pass through the third quadrant. Thus, we realize that its optimal position depends on the location of the points with coordinates $(-1/\kappa_i^A, -\kappa_i^B)$ which must be below the lower branch.

In fact, one can face four distinct possibilities: If the points $(-1/\kappa_i^A, -\kappa_i^B)$ are far enough from the origin and the axes of the coordinate system, then the best bound is obtained when either $t_2 = 0$ or $t_6 = 0$ depending on the location of the points $(3/4\mu_i^A, 4\mu_i^B/3)$ in the first quadrant through which the upper branch passes, see Figure 8. In this situation setting the determinant of the second set of inequalities in (4.59) to zero generates a set of two equations to be solved for t_4 and one of t_6 or t_2, whichever is nonzero. The solution in the former case has the following form

$$t_2 = 0, \quad t_6 = 2\frac{\mu_1^A\mu_2^B - \mu_2^A\mu_1^B}{\mu_1^A - \mu_2^A}, \quad t_4^2 = \frac{\mu_1^B - \mu_2^B}{\mu_1^A - \mu_2^A}, \tag{4.63}$$

and (4.61) becomes a straight line, which defines the bound

$$y_\kappa^B \;\geq\; \frac{2}{3}t_6 + t_4^2\, y_\kappa^A. \tag{4.64}$$

In the latter case the parameters are given by the expressions

$$t_2 = -\frac{1}{2}\frac{\mu_1^A\mu_2^B - \mu_2^A\mu_1^B}{\mu_1^A\mu_2^A(\mu_1^B - \mu_2^B)}, \quad t_6 = 0, \quad t_4^2 = \frac{\mu_1^B\mu_2^B(\mu_1^A - \mu_2^A)}{\mu_1^A\mu_2^A(\mu_1^B - \mu_2^B)}, \tag{4.65}$$

and the bound is described by

$$1/y_\kappa^A \;\geq\; \frac{2}{3}t_2 + t_4^2/y_\kappa^B. \tag{4.66}$$

A simple test can be performed to verify which one of t_2 or t_6 vanishes. Since for a well-ordered composite the values of t_6 in (4.63) and t_2 in (4.65) have opposite signs, one should choose the case that assures positivity of the constants. Notice, that the expressions obtained for the bounds in these two cases are equivalent to the bounds obtained for a badly ordered composite.

The remaining two possibilities occur when the lower branch on its move into the third quadrant hits one of the points with coordinates $(-1/\kappa_i^A, -\kappa_i^B)$. Then the best bound is a hyperbola that passes through three points: the lower branch passes through one of the two points $(-1/\kappa_i^A, -\kappa_i^B)$ such that the other lies below the branch, while the upper branch passes again through the points in the first quadrant with coordinates $(3/4\mu_i^A, 4\mu_i^B/3)$, see Figure 9. Thus, to find the coefficients t_2, t_4 and t_6 a system of three algebraic equations must be solved:

$$\begin{gathered}\left(\frac{1}{2\mu_2^A} - t_2\right)(2\mu_2^B - t_6) = t_4^2, \quad \left(\frac{1}{2\mu_1^A} - t_2\right)(2\mu_1^B - t_6) = t_4^2,\\ \left(\frac{2}{3\kappa_i^A} + t_2\right)\left(\frac{3}{2}\kappa_i^B + t_6\right) = t_4^2,\end{gathered} \tag{4.67}$$

where the index i corresponds to the point in the third quadrant that the hyperbola passes through. The solution has a simpler form if a parametrization parameter ξ is introduced. Then the bound can be represented in the form (2.7). The meaning of this parameter will be clear from the description later in the text, where the microgeometries attaining the bounds are discussed.

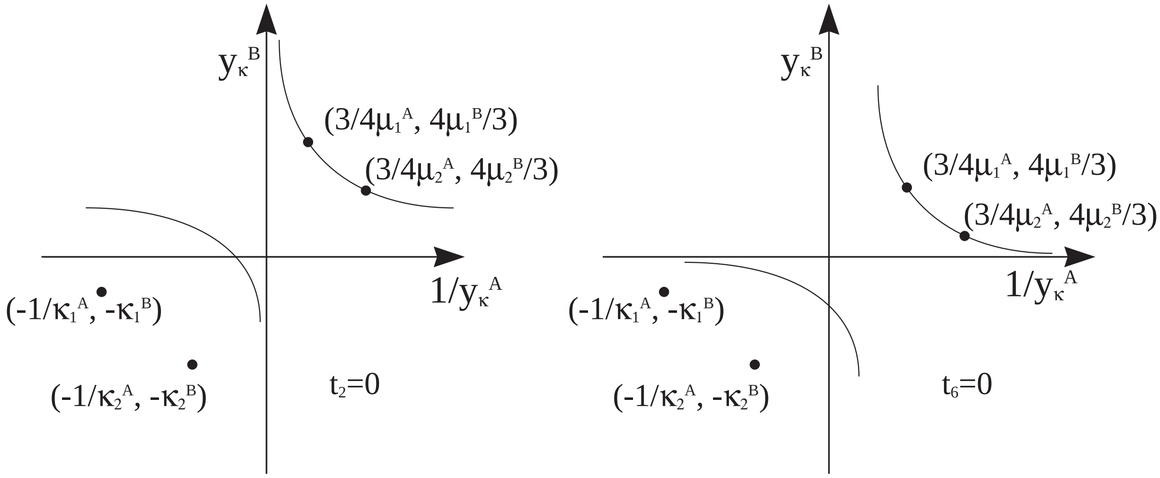

Fig. 8. Location of the optimal hyperbola in the $(1/y_\kappa^A, y_\kappa^B)$ plane which leads to the bound in the well ordered case. The hyperbola passes through the points in the first quadrant that correspond to the Hashin–Shtrikman bounds. The left figure corresponds to the $t_2 = 0$ case when the y_κ^B axis becomes the vertical asymptote of the hyperbola. The figure to the right corresponds to the $t_6 = 0$ case when the $1/y_\kappa^A$ axis becomes the horizontal asymptote of the hyperbola.

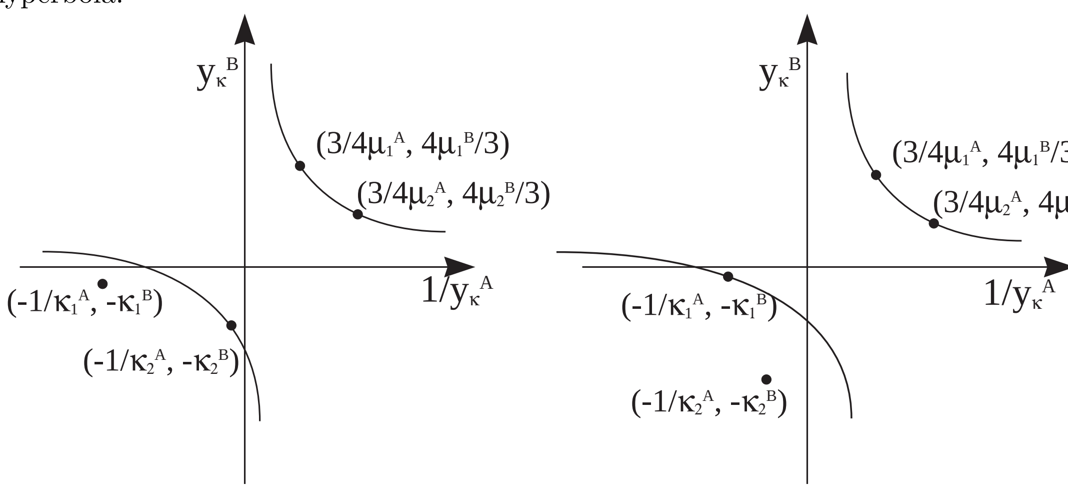

Fig. 9. Location of the optimal hyperbola in the $(1/y_\kappa^A, y_\kappa^B)$ plane which leads to the bound for a well ordered composite. In these two cases the hyperbola passes through the points in the first quadrant that correspond to the Hashin–Shtrikman bounds and one of the points in the third quadrant.

4.2.2 Second mixed bound

The second mixed bound, associated with the minimization of $I_{\zeta\tau}$, provides a lower bound on y_κ^A for fixed y_κ^B but an upper bound on y_κ^B for fixed y_κ^A. The bound is simply obtained by switching the roles of the indices A and B in the procedure just described. However, it should be noted that the decision on which points in the third quadrant are relevant, must be made independently for the first and second mixed bounds. The inequalities derived from the quasiconvexity test remain unchanged. The inequality that defines the bound obtains the form

$$\left(\frac{2}{3y_\kappa^B} - t_2\right)\left(\frac{3}{2}y_\kappa^A - t_6\right) - t_4^2 \geq 0, \tag{4.68}$$

which is a hyperbola in the $(y_\kappa^A, 1/y_\kappa^B)$ plane. Similar to the previous case of the lower bound, the optimal hyperbola corresponds to decreasing t_2 and t_6 towards zero if there are no points in the third quadrant that could prevent this. It is no wonder that the expressions for the second mixed bound faithfully copy those for the first mixed bound with the only difference being in the inequality sign.

Thus, the simplest way to obtain the bounds is to evaluate the four curves defined by (4.64) and (4.66) and those by (2.7) and choose the least restrictive pair, or in other words, the outermost pair of curves.

5 Microgeometries

In this section we describe microgeometries that are found to attain points on the coupled bounds for the immediate and relaxed effective bulk moduli. These microgeometries are based on the microgeometries found to attain bounds on the conductivity of symmetric materials (Schulgasser, 1977), on coupled conductivity bounds and bounds on the complex conductivity (Milton, 1981a,b). First, let us note that in all the cases described above, the bounds enclose a lens-shaped region with the vertex points P_1 and P_2, that correspond to the Hashin–Shtrikman bounds for which the microgeometry is a well-known coated sphere assemblage (Hashin, 1962). Namely, the point P_1 with coordinates $(4\mu_1^A/3, 4\mu_1^B/3)$ corresponds to an assemblage by filling the domain with composite spheres of various sizes ranging to the infinitesimal with phase 2 as a core and phase 1 as a coating, while the point $P_2 = (4\mu_2^A/3, 4\mu_2^B/3)$ is obtained by switching the phase ordering: phase 1 becomes the core surrounded by a coating of phase 2. The radii of the core and the shell are chosen such that their materials occupy the given volume fractions in each composite sphere.

For microgeometries that attain the correlated bounds in the middle range between the vertex points, we consider two potential classes of microgeometries that have been found to attain various coupled bounds. The first microgeometry is a doubly coated sphere assemblage which is constructed as follows: One starts with a composite sphere made of a spherical core of material 1 surrounded by a spherical shell of phase 2. Then the obtained composite sphere is surrounded again by a coating of phase 1 and space is filled with these doubly coated spheres of various sizes ranging to the infinitesimal. Let us define a parameter ξ $(0 \leq \xi \leq 1)$ that indicates the position of the middle shell made of phase 2. It denotes what proportion of the volume of the phase 1 is stored in the core, such that $\xi = 0$ corresponds to when the radius of the core is zero and phase 2 becomes the core, while $\xi = 1$ implies that the shell 2 is at the outer radius of the composite sphere and the external coating 1 vanishes. In both the cases the doubly coated sphere assemblage reduces to the composite sphere assemblage of Hashin. Straightforward calculation yields the following expression for the bulk component of the Y-tensor:

$$y_\kappa(\xi) = \frac{4}{3}\frac{f_2\mu_1\left(3\kappa_1+4\mu_2\right)(1-\xi)+\left(3\kappa_1+4\mu_1\right)\mu_2\xi}{f_2\left(3\kappa_1+4\mu_2\right)(1-\xi)+\left(3\kappa_1+4\mu_1\right)\xi}. \tag{5.1}$$

The values y_κ^A and y_κ^B evaluated for the composite at states A and B, respectively, for ξ varying in the range between 0 and 1 and plotted versus each other provides a curve correlating the immediate and relaxed bulk moduli for the described microgeometry. The curve is indicated in Figures 1–2 by one of the dashed lines. It is interesting to note that this parameterized relation coincides with the bound obtained from the solution of equations (4.67), where the lower branch of the hyperbola passes though the point $(-1/\kappa_1^A, -\kappa_1^B)$ in the third quadrant.

Analogously, switching phases in the described microgeometry leads to an assemblage of doubly coated spheres each having a core of phase 2 coated by a spherical shell of phase 1 which is in turn coated by an outer shell of phase 2. The result for the effective bulk modulus of this microgeometry is obtained by switching phase indexes 1 and 2 in the parameterized equation (5.1). Similar to the previous case it corresponds to the case when the lower branch of the hyperbola passes though the point $(-1/\kappa_2^A, -\kappa_2^B)$ in the third quadrant. It is also clear that the upper bound corresponds to this or the other microgeometry if the optimal hyperbola in $(y_\kappa^A, 1/y_\kappa^B)$ plane crosses one of the points with coordinates $(-\kappa_1^A, -1/\kappa_1^B)$ or $(-\kappa_2^A, -1/\kappa_2^B)$ in the third quadrant of the coordinate system. Thus, in these cases the bounds correspond to the known microgeometries of doubly coated spheres and hence they are optimal.

In the remaining case of the well ordered composite and in the badly ordered case, where the points in the third quadrant are irrelevant from the point of view of optimal bounds, some isolated points on the bounds correspond to known microgeometries. To describe the microgeometries, let us first construct a laminated material of phases 1 and 2. The components of the effective stiffness tensor of the laminate are given by Backus's formulas (Backus, 1962):

$$\begin{aligned}
&C_{1111} = \langle 1/(\lambda+2\mu)\rangle^{-1}, \quad C_{1212} = \langle 1/\mu\rangle^{-1}, \quad C_{2323} = \langle\mu\rangle \\
&C_{1122} = C^*_{1133} = \langle\lambda/(\lambda+2\mu)\rangle\langle 1/(\lambda+2\mu)\rangle^{-1} \\
&C_{2222} = C^*_{3333} = \langle 4\mu(\lambda+\mu)/(\lambda+2\mu)\rangle + \langle 1/(\lambda+2\mu)\rangle^{-1}\langle\lambda/(\lambda+2\mu)\rangle^2 \\
&C_{2233} = \langle 2\mu\lambda/(\lambda+2\mu)\rangle + \langle 1/(\lambda+2\mu)\rangle^{-1}\langle\lambda/(\lambda+2\mu)\rangle^2,
\end{aligned} \tag{5.2}$$

where $\lambda = \kappa - 2\mu/3$ is the Lamé modulus. The next step of the microgeometry construction is to use Schulgasser's procedure (Schulgasser, 1977) of building an isotropic polycrystal by combining rotated plies of the laminate with moduli (5.2). This procedure was extended to the effective bulk modulus of isotropic polycrystals by Avellaneda and Milton (1989) who showed that there are special microstructures that attain the Voigt-Reuss-Hill bounds on the effective bulk modulus:

$$\kappa_R \le \kappa_* \le \kappa_V, \quad \text{where} \quad \kappa_V = \{\boldsymbol{\mathcal{C}}\}_{iijj}/9, \quad \kappa_R \le 1/\{\boldsymbol{\mathcal{C}}^{-1}\}_{iijj}, \tag{5.3}$$

where $\boldsymbol{\mathcal{C}}$ is given by (5.2). A straightforward calculation shows that these sharp bounds when expressed in terms of the bulk component of the Y-tensor reduce to

$$\frac{4}{3}\frac{\mu_1\mu_2}{f_1\mu_1 + f_2\mu_2} \le y_\kappa \le \frac{4}{3}(f_2\mu_1 + f_1\mu_2). \tag{5.4}$$

These bounds evaluated for the states A and B provide two points P_5 and P_6 in the (y^A_κ, y^B_κ) plane. The point P_5 has coordinates of the Voigt bound

$$P_5 = \left(\frac{4}{3}(f_2\mu_1^A + f_1\mu_2^A), \frac{4}{3}(f_2\mu_1^B + f_1\mu_2^B)\right),$$

which lies on the straight line between the Hashin–Shtrikman points described by equation (2.4). The second point P_6 has coordinates of the Reuss bound

$$P_6 = \left(\frac{4}{3}\frac{\mu_1^A\mu_2^A}{f_1\mu_1^A + f_2\mu_2^A}, \frac{4}{3}\frac{\mu_1^B\mu_2^B}{f_1\mu_1^B + f_2\mu_2^B}\right), \tag{5.5}$$

and lies on the hyperbola (2.5).

There are two additional points P_3 and P_4 lying on the bound represented by a straight line between the Hashin–Shtrikman points in the Y-plane. They are obtained by constructing the isotropic polycrystal with the effective bulk modulus given by the Voigt bound using a transversely isotropic composite cylinder assemblage as the basic material instead of the laminate. For instance, an assemblage of composite cylinders with the phase 2 as a cylinder core surrounded by matrix shell 1 leads to the following point

$$P_3 = \left(\mu_1^A + \frac{1}{3}(f_1\mu_2^A + f_2\mu_1^A), \;\; \mu_1^B + \frac{1}{3}(f_1\mu_2^B + f_2\mu_1^B)\right). \tag{5.6}$$

The second point P_4 is obtained by switching the location of the phases with corresponding switching of indexes 1 and 2 in the expression above. It turns out that the microgeometries obtained as a result of the assemblage of inserting the composite cylinders into the polycrystalline structure with the Reuss bulk modulus do not attain our bounds.

Acknowledgements

We gratefully acknowledge the support of the University of Utah and the National Science Foundation under grants DMS-0108626 and DMS-0411035 and V. Vinogradov is additionally thankful for support from the Army Research Office through grant No. 41363-MA.

References

Avellaneda, M., Milton, G. W., 1989. Optimal bounds on the effective bulk modulus of polycrystals. SIAM Journal on Applied Mathematics 49 (3), 824–837.

Backus, G. E., 1962. Long-wave elastic anisotropy produced by horizontal layering. Journal of Geophysical Research 67 (11), 4427–4440.

Bergman, D. J., 1978a. Analytical properties of the complex effective dielectric constant of a composite medium with applications to the derivation of rigorous bounds and to percolation problems. In: Garland, J. C., Tanner, D. B. (Eds.), Electrical Transport and Optical Properties of Inhomogeneous Media. Vol. 40. American Institute of Physics, Woodbury, New York, pp. 46–61, ISBN 0-88318-139-8.

Bergman, D. J., 1978b. The dielectric constant of a composite material — A problem in classical physics. Physics Reports 43 (9), 377–407.

Bergman, D. J., 1982. Rigorous bounds for the complex dielectric constant of a two-component composite. Annals of Physics 138 (1), 78–114.

Berryman, J. G., Milton, G. W., 1988. Microgeometry of random composites and porous media. Journal of Physics D: Applied Physics 21, 87–94.

Cherkaev, A. V., 2000. Variational Methods for Structural Optimization. Vol. 140. Springer-Verlag, Berlin, ISBN 0-387-98462-3.

Cherkaev, A. V., Gibiansky, L. V., 1992. The exact coupled bounds for effective tensors of electrical and magnetic properties of two-component two-dimensional composites. Proceedings of the Royal Society of Edinburgh. Section A, Mathematical and Physical Sciences 122 (1–2), 93–125.

Cherkaev, A. V., Gibiansky, L. V., 1993. Coupled estimates for the bulk and shear moduli of a two-dimensional isotropic elastic composite. Journal of the Mechanics and Physics of Solids 41 (5), 937–980.

Cherkaev, A. V., Gibiansky, L. V., 1994. Variational principles for complex conductivity, viscoelasticity, and similar problems in media with complex moduli. Journal of Mathematical Physics 35 (1), 127–145.

Christensen, R. M., 1971. Theory of Viscoelasticity: an Introduction. Academic Press, New York, ISBN 0-12-174250-4.

Clark, K. E., Milton, G. W., 1995. Optimal bounds correlating electric, magnetic and thermal properties of two-phase, two-dimensional composites. Proceedings of the Royal Society of London. Series A, Mathematical and Physical Sciences 448 (1933), 161–190.

Francfort, G. A., Milton, G. W., 1994. Sets of conductivity and elasticity tensors stable under lamination. Communications on Pure and Applied Mathematics (New York) 47 (3), 257–279.

Francfort, G. A., Murat, F., 1986. Homogenization and optimal bounds in linear elasticity. Archive for Rational Mechanics and Analysis 94 (4), 307–334.

Gibiansky, L. V., Milton, G. W., 1993. On the effective viscoelastic moduli of two-phase media. I. Rigorous bounds on the complex bulk modulus. Proceedings of the Royal Society of London. Series A, Mathematical and Physical Sciences 440 (1908), 163–188.

Gibiansky, L. V., Milton, G. W., Berryman, J. G., 1999. On the effective viscoelastic moduli of two-phase media: III. Rigorous bounds on the complex shear modulus in two dimensions. Proceedings of the Royal Society of London. Series A, Mathematical and Physical Sciences 455 (1986), 2117–2149.

Gibiansky, L. V., Torquato, S., 1993. Link between the conductivity and elastic moduli of composite materials. Physical Review Letters 71 (18), 2927–2930.

Gibiansky, L. V., Torquato, S., 1995. Rigorous link between the conductivity and elastic moduli of fibre-reinforced composite materials. Philosophical Transactions of the Royal Society of London Series A 353, 243–278.

Gibiansky, L. V., Torquato, S., 1996a. Connection between the conductivity and bulk modulus of isotropic composite materials. Proceedings of the Royal Society of London. Series A, Mathematical and Physical Sciences 452 (1945), 253–283.

Gibiansky, L. V., Torquato, S., 1996b. Phase-interchange relations for the elastic moduli of two-phase composites. International Journal of Engineering Science 34 (7), 739–760.

Golden, K., Papanicolaou, G., 1983. Bounds for effective parameters of heterogeneous media by analytic continuation. Communications in Mathematical Physics 90 (4), 473–491.

Hashin, Z., 1962. The elastic moduli of heterogeneous materials. J. Appl. Mech. 29, 143–150.

Hashin, Z., 1970a. Complex moduli of viscoelastic composites – i. general theory and application to particulate composites. International Journal of Solids and Structures 6, 539–552.

Hashin, Z., 1970b. Complex moduli of viscoelastic composites – ii. fiber reinforced materials. International Journal of Solids and Structures 6, 797–807.

Hashin, Z., 1983. Analysis of composite materials — A survey. Applied Mechanics Reviews 50, 481–505.

Hashin, Z., Shtrikman, S., 1962. A variational approach to the theory of the effective magnetic permeability of multiphase materials. Journal of Applied Physics 33, 3125–3131.

Hashin, Z., Shtrikman, S., 1963. A variational approach to the theory of the elastic behavior of multiphase materials. Journal of the Mechanics and Physics of Solids 11, 127–140.

Kantor, Y., Bergman, D. J., 1984. Improved rigorous bounds on the effective elastic moduli of a composite material. Journal of the Mechanics and Physics of Solids 32, 41–62.

Lurie, K. A., Cherkaev, A. V., 1984. Exact estimates of conductivity of composites formed by two isotropically conducting media taken in prescribed proportion. Proceedings of the Royal Society of Edinburgh. Section A, Mathematical and Physical Sciences 99 (1–2), 71–87.

Lurie, K. A., Cherkaev, A. V., 1986. Exact estimates of the conductivity of a binary mixture of isotropic materials. Proceedings of the Royal Society of Edinburgh. Section A, Mathematical and Physical Sciences 104 (1–2), 21–38.

Milton, G. W., 1981a. Bounds on the complex permittivity of a two-component composite material. Journal of Applied Physics 52 (8), 5286–5293.

Milton, G. W., 1981b. Bounds on the transport and optical properties of a two-component composite material. Journal of Applied Physics 52 (8), 5294–5304.

Milton, G. W., 1990a. A brief review of the translation method for bounding effective elastic tensors of composites. In: Maugin, G. A. (Ed.), Continuum Models and Discrete Systems. Vol. 1. Longman Scientific and Technical, Harlow, Essex, United Kingdom, pp. 60–74, ISBN 0-582-05121-5.

Milton, G. W., 1990b. On characterizing the set of possible effective tensors of composites: The variational method and the translation method. Communications on Pure and Applied Mathematics (New York) 43 (1), 63–125.

Milton, G. W., 1994. A link between sets of tensors stable under lamination and quasiconvexity. Communications on Pure and Applied Mathematics (New York) 47 (7), 959–1003.

Milton, G. W., 2002. The Theory of Composites. Cambridge University Press, Cambridge, UK, ISBN 0-521-78125-6.

Milton, G. W., Berryman, J. G., 1997. On the effective viscoelastic moduli of two-phase media. II. Rigorous bounds on the complex shear modulus in three dimensions. Proceedings of the Royal Society of London. Series A, Mathematical and Physical Sciences 453 (1964), 1849–1880.

Milton, G. W., Cherkaev, A. V., 1995. Which elasticity tensors are realizable? ASME Journal of Engineering Materials and Technology 117, 483–493.

Milton, G. W., Phan-Thien, N., 1982. New bounds on effective elastic moduli of two-component materials. Proceedings of the Royal Society of London. Series A, Mathematical and Physical Sciences 380, 305–331.

Murat, F., Tartar, L., 1985. Calcul des variations et homogénísation. (French) [Calculus of variation and homogenization]. In: Les méthodes de l'homogénéisation: théorie et applications en physique. Vol. 57 of Collection de la Direction des études et recherches d'Électricité de France. Eyrolles, Paris, pp. 319–369, english translation in *Topics in the Mathematical Modelling of Composite Materials*, pp. 139–173, ed. by A. Cherkaev and R. Kohn, ISBN 0-8176-3662-5.

Nesi, V., Rogora, E., 2004. A search for compensated compactness at its best, in preparation.

Prager, S., 1969. Improved variational bounds on some bulk properties of a two-phase random medium. Journal of Chemical Physics 50, 4305–4312.

Schulgasser, K., 1977. Bounds on the conductivity of statistically isotropic polycrystals. Journal of Physics C: Solid State Physics 10, 407–417.

Tartar, L., 1979a. Compensated compactness and applications to partial differential equations. In: Knops, R. J. (Ed.), Nonlinear Analysis and Mechanics, Heriot-Watt Symposium, Volume IV. Vol. 39 of Research Notes in Mathematics. Pitman Publishing Ltd., London, pp. 136–212.

Tartar, L., 1979b. Estimation de coefficients homogénéisés. (French) [Estimation of homogenization coefficients]. In: Glowinski, R., Lions, J.-L. (Eds.), Computing

Methods in Applied Sciences and Engineering: Third International Symposium, Versailles, France, December 5–9, 1977,. Vol. 704 of Lecture Notes in Mathematics. Springer-Verlag, Berlin, pp. 364–373, english translation in *Topics in the Mathematical Modelling of Composite Materials*, pp. 9–20, ed. by A. Cherkaev and R. Kohn. ISBN 0-8176-3662-5.